AGGREGATE PIERS: STRESS TRANSFER MECHANISM AND CONSTRUCTION EFFECT

by

William Gamboa

A thesis submitted in partial fulfillment
of the requirements for the degree

of

Master of Science

in

Civil Engineering

MONTANA STATE UNIVERSITY
Bozeman, Montana

December 9, 2022

DEDICATION

I dedicate this thesis to my parents William Gamboa Vasquez and Gaby Ellis Leandro and my wife Rosa Rodriguez Badilla, who have supported me in all walks of my life and through the entire duration of my master's degree. I wish to express my deepest gratitude to them for helping me make my dream come true. I appreciate them for their unconditional support and love that they have always showered on me.

ACKNOWLEDGEMENTS

My foremost thanks must go to my advisor Prof. Mohammad Khosravi for his technical advice, guidance and for his support during my Master's. journey. He offered unwavering support and devoted many hours to me in reviewing my manuscripts. I would also like to express my sincere appreciation to the members of the supervisory committee, comprising Professor Kirsten Matteson and Professor Michael Berry. My research at Montana State University was sponsored by Specialty Foundation Systems, LLC. The support is greatly appreciated. I will always be thankful to Coby Burns and Taj Mukadam for their support and help.

TABLE OF CONTENTS

1. CHAPTER ONE: GENERAL INTRODUCTION 1

Overview 1
Objectives and Scope 2
Organization of the Thesis.....3

2. CHAPTER TWO: BACKGROUND 5

General Literature Review.....5
Behavior of Axially Loaded Aggregate Piers.....6
Single Isolated Aggregate Piers 6
Group of Aggregate Piers 7
Numerical Modeling of Aggregate Piers.....8
Field Testing of Aggregate Piers 10
Single Aggregate Piers 10
Group of Aggregate Piers 12
Summary of Literature Review.....13
Summary.....13
Outstanding Problems and Issues.....14

3. CHAPTER THREE: FIELD EXPERIMENT AND NUMERICAL MODELING

OF A SINGLE AGGREGATE PIER 15

Introduction.....15
Overview of Field Load Tests 17
Overview of the Numerical Simulations 20
Numerical Results and Parametric Analyses.....21

4. CHAPTER FOUR: STRESS TRANSFER MECHANISM AND

CONSTRUCTION EFFECT OF END-BEARING AGGREGATE PIERS.....27

Introduction.....27
Site Geotechnical Investigation 29
An Overview of the Experimental Program 30
Test Results.....33

TABLE OF CONTENTS CONTINUED

Bearing Pressure Displacement (q-δ) Behavior of Single and Group Aggregate Piers 33
Vertical Stress Distributions 35
Effect of In-Situ Properties on Response of Aggregate Piers 36
Comparison of q-δ Behavior of Aggregate Piers 36
Stress Distributions along the Depth of Aggregate Piers 38
Group Effect 39
Group Efficiency 40
Stress Concentration 41
Pier Stiffness 44
Construction Effect 46

5. CHAPTER FIVE: SUMMARY AND CONCLUSIONS 62

Recommendations for Further Study 64

REFERENCES CITED 65

APPENDICES 72
APPENDIX A: Pictures of the Full-Scale Field Test Construction Process 73

LIST OF TABLES

Table Page

1. Parameters for the soils and aggregate pier in the baseline model.....23

2. Previous studies of aggregate piers 51

3. Material used to build the aggregate piers 54

4. ANOVA Analysis for CPT tip resistance, Footing Test.....61

5. ANOVA Analysis for CPT tip resistance, Single Pier Test.....61

LIST OF FIGURES

Figure Page

1. a) Schematic of upper and lower zones (Geopier® Manual), b) Aggregate pier construction process (Geopier® Manual) 23

2. a) The location of the proposed garage (taken from Google Earth), b) Variation of SPT N values with depth 23

3. a) Sketch and b) Photo of the experimental load test setup 24

4. Grain size distribution of aggregate pier materials 24

5. Load-deflection results obtained during field load tests 25

6. Numerical model configuration of the baseline model 25

7. Deflection curves for site testing and numerical analysis 26

8. a) Effect of the aggregate friction angle on the load-displacement response of aggregate piers, b) Lateral displacement at 1m from ground surface 26

9. Stress distribution between aggregate pier and surrounding soil a) Group of piers under footing; b) Single pier 51

10. Settlement analysis procedure 52

11. CPT initial conditions 52

12. Schematic of the full-scale load test 53

13. Schematic of the single pier load test 53

14. Tell-tale reference plate 54

15. Measured load-settlement curves for: a) Single pier test; b) Concrete footing test 54

6. Comparison of the measured Load-Settlement Curves for: a) Footing Test; b) Single Pier Test 55

17. Comparison of CPT initial conditions 55

LIST OF FIGURES CONTINUED

Figure Page

18. Group efficiency 56

19. Vertical stress distribution: a) Single pier; b) Footing test 56

20. Vertical stress increase at each load cell a) Footing test; b) Comparison 57

21. Single pier vertical stress increase at each load cell 57

22. Stress concentration effect: a) Stress concentration b) Stress concentration ratio 58

23. Pier stiffness ratio 58

24. Inclinometer lateral deformation after installation a) Single pier test; b) Concrete footing. 59

25. Comparison of lateral displacement after construction 59

26. CPT prior and after installation of single aggregate pier 60

27. CPT prior and after installation of group of aggregate piers 60

ABSTRACT

This thesis is a compilation of two different papers based on the behavior of aggregate piers which is a soil improvement method used to increase the bearing capacity and reduce the expected settlements of soils in which different types of structures are supported.

The first paper describes the results of two modulus load tests and a dimensional finite difference analysis (FDA) conducted to evaluate the load-displacement response of isolated aggregate piers. Load test aggregate piers were constructed with two different materials: the first one with 38 mm base coarse and the second one with 75 mm subbase coarse materials. The numerical analyses provided reasonable predictions of the load-displacement response of the isolated aggregate piers. Parametric analyses using the validated numerical model illustrate that the lateral stress increment on the soil around the pier during the installation process of the pier should be considered in the numerical analysis, otherwise the settlement can be overestimated.

The second paper is based on two full-scale load tests that were conducted to examine the load transfer mechanisms of end-bearing single and group aggregate piers. The first included a load test on a 0.76 m diameter isolated aggregate pier. The length of the aggregate pier was 4.3 m. The second test included a 2.1 m square reinforced concrete footing supported by four 0.76 m diameter aggregate piers of 4.3 m long. The soil consists of soft to medium stiff layers of sandy and clayey silt overlain by a 2-m-thick, softer silty clay layer. At the bottom, weathered rock was found. The load transfer mechanism within the length of the piers was examined using a series of load cells and tell-tale reference plates installed at different depths of the aggregate piers. Additionally, the installation effect was investigated using Cone Penetration Tests (CPT) conducted prior and after construction of the aggregate piers and inclinometers installed at multiple locations around the aggregate piers. The results of the experiments were compared with those in the literature to provide insights on the performance of aggregate piers with different configurations (single vs. group) and depths (floating vs end-bearing) in different soil profiles.

CHAPTER ONE: GENERAL INTRODUCTION

Overview

Construction over highly compressible soils can create excessive settlement and bearing capacity problems. To overcome these difficulties, deep foundation elements such as driven piles or drilled shafts have been traditionally used to transfer the surcharge loads exerted by the superstructures to a deeper, more competent layer. Although deep foundation methods have proven to be effective in most cases, these methods are expensive and typically slow to build.

As alternatives to deep foundation methods, ground improvement technologies have been widely used to improve the load bearing capacity and stiffness of the soil layers located immediately underneath the superstructures. According to Mitchell (1981), basic concepts of ground improvement such as drainage, densification, cementation, and reinforcement were developed hundreds or even thousands of years ago.

Although the basic principles of ground improvement have been unchanged since the early days, the practices have been changing with time owing to the development of new materials, machinery, and technologies. In the past, soil improvement technologies have mainly focused on the development of vibratory methods for densification of cohesionless soils, injection and grouting materials and procedures, and new concepts of soil reinforcement (Mitchell, 1981).

Among other soil reinforcement technologies, aggregate pier systems have been emerging rapidly during the last three decades to become one of the most popular methods for stiffening and stabilizing soft soils, not only in the United States but around the world. Aggregate piers technology was developed in the early 1980s to provide an economical alternative to deep foundations and traditional methods of soil improvement such as over-excavation and

replacement. Aggregate piers are considered floating foundation systems consisting of a stiff composite layer, typically to a minimum depth equal to the stress influence zone of the footing, to reduce the applied pressure on the soil matrix and foundation settlement.

Objectives and Scope

The primary objectives of this research were to: (1) compare the results of a full-scale test on a single aggregate pier to the results obtained by the finite difference analysis (FDA) software to investigate the load-transfer mechanism and the influence of material on the construction of the aggregate pier; (2) investigate, through full-scale load tests, the load-transfer mechanism and the interaction of both isolated aggregate piers and groups of aggregate piers with matrix soil; (3) investigate the construction effect through the use of cone penetration tests (CPTs) and inclinometer readings before and after construction of aggregate piers.

One square reinforced concrete footing supported by four aggregate piers and one isolated aggregate pier were constructed in the Marga Hosaeus Fitness Center at Montana State University in Bozeman, Montana. The footing width was 2.10 m, and the thickness was 0.60 m. All piers in the pier groups were 0.76 m in diameter with a length of 4.30 m. One of the four piers in the group of piers was instrumented with 4 load cells and 4 tell-tale reference plates. One isolated pier of 0.76 m in diameter and 4.30 m in length was installed near the trial pier-supported footing. The isolated pier was equipped with three load cells and three tell-tale reference plates and covered with a 25.4 mm thick steel plate.

Prior to the construction of the footing and isolated piers, comprehensive in-situ and laboratory testing programs were implemented. In-situ tests included the standard penetration test (SPT) and cone penetration test (CPT). Laboratory tests conducted on undisturbed soil samples

collected from the construction site included soil indices and one-dimensional consolidation tests. Full scale load tests were conducted on the trial footings and on the isolated piers. Instrumentation includes load cells, tell-tale steel plates and inclinometer casing. Readings from the load cells, tell-tales and inclinometers were taken simultaneously.

To compare the load test and the finite difference analysis, an axisymmetric element model was developed using the computer program Flac (2D version) to model the isolated aggregate piers. Model parameters were estimated from the laboratory and the in-situ tests performed during the construction of that load test. The pier installation process was modeled as an expanding cavity increasing the k_o value of the surrounding soil in which boundary conditions were estimated from field measurements.

Organization of the Thesis

The thesis is divided into five different chapters. Chapter one presents a general introduction, chapter two includes background and general literature review, chapters three and four are a compilation of one paper published for the 2022 Geotechnical Congress and one paper submitted to a scholarly geotechnical engineering journal including more specific references to literature reviewed, research data, and significant findings, and chapter five presents conclusions that summarize significant research findings and directions for future research.

Chapter three presents a numerical analysis using an axisymmetric, finite difference model study performed to investigate the influence of induced lateral stress on shear strength and vertical stiffness. This analysis is also used to investigate the effect of the grain size and friction angle of the aggregate pier on the settlement obtained during the application of a vertical compressive load.

Chapter four presents the results from full-scale, instrumented load tests conducted on one trial square pier-supported footings and one isolated aggregate pier. Group effects are investigated by comparing the behavior of an individual pier within the pier group and an isolated pier from the same diameter and length. Evaluation of the current design method is carried out by comparing the calculated parameters with the measured values.

CHAPTER TWO: BACKGROUND

General Literature Review

Since their inception, aggregate piers have been used to support a wide range of structures, including structures supported by isolated or strip footings, highway embankments, slabs, retaining walls, and storage tanks (Lawton and Fox, 1994; White and Suleiman, 2004; Minks et al., 2001; Wissmann et al., 2002; Wong et al., 2004; Wissmann et al., 2001).

Typical applications of aggregate pier systems include settlement control and bearing capacity improvement. Construction procedures for aggregate piers are well described in the literature (Lawton and Fox, 1994; Lawton et al., 1994). The standard construction procedure includes backfilling and compacting successive thin layers of base-coarse aggregate in a pre-bored cavity using a beveled tamper connected to a low amplitude, high frequency hydraulic hammer. The aggregate is compacted by impact energy rather than vibrating energy. As a result of ramming, the backfilling aggregate is pushed laterally along the shaft and vertically at the bottom of the cavity, thereby pre-stressing and pre-straining the matrix soil adjacent to the cavity wall (Fox and Cowell, 1998).

Although successful performances of aggregate pier systems have been well documented (Lawton and Fox, 1994; Lawton et al., 1994; White et al., 2002), insights into the load-transfer mechanism of the piers, the pier-soil interaction and the construction effect have yet to be elucidated, especially for end bearing supported aggregate piers.

According to the design basics of the system, since aggregate piers are relatively short and generally not intended to penetrate to a competent layer, the aggregate pier system is essentially a

floating system in which the surcharge load will have to be dissipated mostly through the pier-soil interfacial friction.

The additional lateral stress induced from pier installation not only provides more confinement around the pier, which subsequently improves the interfacial friction, but also may alter the behavior of the matrix soil itself (Stuedlein, 2008). There is a lack of information about how the installation process changes the mechanical properties of the soil beyond just creating a lateral displacement on the surrounding soil. To gain insight into the complex pier-soil interaction and the impact of the pier installation on soil behaviors, several research projects were conducted, using both experimental (Handy and White, 2006) and especially numerical approaches (Algin and Gumus, 2018; Halabian and Shamsabadi, 2014). Table 1 includes a general list of some of the most important research projects for both stone columns and aggregate piers used as reference for the present study for both field and numerical analyses. Table 3 show research projects specific for aggregate piers used in that chapter. The design and behavior of aggregate piers and stone columns is not the same, but they have similar design principles that can be applied to both systems. The results obtained from these research projects have established the elements for this thesis.

Behavior of Axially Loaded Aggregate Piers

Single Isolated Aggregate Piers

The behavior of axially loaded aggregate piers is not as well understood as compared to more common and older forms of ground improvement (e.g., excavation and replacement, preload and surcharge, etc). An aggregate pier, composed of a cohesionless material, derives its strength

from lateral confinement (Geopier® Manual). The confinement on a column is provided by the native soil, the amount of which is limited by the strength of the native soil (Stuedlein, 2008). Since the aggregate pier is stiffer than the native soil, vertical stresses will concentrate within the pier with a corresponding decrease in vertical stress within the surrounding soil. As the load is redistributed within the composite soil system, the column and surrounding soil will deform until force equilibrium is reached (Stuedlein, 2008). In normally consolidated native soils, the loaded soil-column system consolidates and gains strength as excess pore water pressures within the softer, cohesive soil are relieved through the radial drainage provided by the piers. In overconsolidated soils, the soil-column system strains with elastic and plastic components to redistribute the applied load (Handy, 2006).

Vertical loading of a single aggregate pier may produce failure of the pier through one of two general modes. If the concentrated load applied to the stone column exceeds the strength generated by the lateral confinement of the surrounding soil, plastic flow (deformation) will occur within the column, exhibited by columnar bulging. The second mode of column failure is by shear action along the interface of the pier and the surrounding soil and at the base of the pier, similar to the failure behavior observed in pile foundations (Stuedlein, 2008).

Group of Aggregate Piers

The behavior of axially loaded aggregate pier groups is less understood than the behavior of a single aggregate pier. Difficulties arise, similar with single piers, in the understanding of behavior due to the contrast of stiffness between the introduced aggregate and the native soil and nonlinearity of stress-strain response as compared to stiffer inclusions (e.g., piles). Model tests have, however, provided qualitative insight into the likely behavior of group aggregate piers. For

loading by a rigid plate or footing, the location of an aggregate pier relative to both its neighbor and the center of a footing appears to control the behavior of an aggregate pier within the group (Wood et al, 1997; Wood et al., 2000). A pier along the outer edge of a footing that is not prevented from expanding into the surrounding soil under load will likely fail by the bulging mechanism, similar to a loaded single pier. Moving closer to the center of a loaded footing, a pier may be subject to some amount of confinement. The distribution of stresses due to loading by a more flexible plate or footing is not well studied.

Piers that are "floating" in the native soil (i.e., not founded on a bearing layer) and are relatively short create a potential situation where load cannot be sufficiently shed along the side of the pier shaft, so it is transmitted to the base of the pier. Excessive deformation may result due to the composite system strain and the strains within the native soil receiving transmitted loads. Finally, where the strength of the native soil is extremely weak, the lateral flow of the native soil around a pier may induce lateral loading of the column at the footing edges and result in behavior analogous to lateral loading of piles (Stuedlein, 2008).

Numerical Modeling of Aggregate Piers

The first use of numerical models to predict the behavior of aggregate pier reinforced ground was by Balaam et al. (1976), further expanded by Balaam et al. (1977) and Balaam and Poulos (1983). Finite elements are used to predict the magnitude of ground settlement, whereas finite difference methods are utilized for the prediction of time-rate of settlement. In their formulation, the authors treat the model domain within the unit-cell framework for both finite element and finite difference computations. The inherent implication is that the method is applicable for loading over a wide area.

Barskdale and Bachus (1983a) present an elasto-plastic finite element study considering the unit cell geometry, with elastic boundaries and stress dependent properties for the aggregate. The boundaries of the model were considered to allow possible lateral heave of soft cohesive soil. The boundaries were modeled with elements having a one-inch thickness with a Young's modulus of 0.08 or 6.9 MPa. By the authors' own admission, the approach they selected should be considered for only preliminary engineering. The stone was modeled with a peak angle of internal friction of 42 degrees; the coefficient of lateral earth pressure for both soils were specified at 0.75. Based on these findings, the authors conclude that non-linear theory returns settlements smaller than observed.

Ashmawy, et al (2000) conducted parametric studies using FLAC, a finite difference numerical modeling package, considering an axisymmetric model geometry. The study produced largely unsatisfactory results due to a variety of reasons, including poor representation of the interface of in-situ soil and column, the use of simple Mohr-Coulomb plasticity, poor selection of friction angle and Poisson's ratio for both constituent soils, and the decision to model the unit cell base boundary as rigid. The parametric studies considering variations in Young's modulus, presented on a normalized basis, show very little sensitivity to the Young's modulus. Further, the models overpredict settlements as compared to the field tests conducted on silty and clayey sand by up to 33 percent. Nonetheless, these results provide insight towards developing a more complicated numerical model.

Field Testing of Aggregate Piers

Single Aggregate Piers

Bergado et al. (1987a) investigated the behavior of single aggregate pier reinforced soil by means of six field load tests. The native soil is typically characterized by an overconsolidated, weathered crust 2 m in thickness over very soft, normally consolidated clay. The plastic limit of the soft clay ranges from 30 % to 40 %, the liquid limit from 80 % to 110 %, with natural water content near the liquid limits. The in-situ shear strength as determined by field vane ranged from 30 to 40 kPa for the crust and 15 to 25 kPa for the soft clay. Gravel was used for the aggregate pier material, placed in piers 0.3 m in diameter and 8 m in length. The study included six field tests. The circular footing diameters were 0.3, 0.45, 0.6, 0.75, 0.9, and 1.2 m, providing area replacement ratios of 100, 44, 25, 16, 11, and 6 percent. It was found that the settlement decreased as the size of the footing increased for the same amount of applied load. Bergado et al. (1987b) continued the investigation of the behavior of single aggregate pier reinforced soil with different composition of granular materials and densities by means of 13 field load tests. The aggregate piers were constructed to be 0.3 m in diameter and 8 m in length. The aggregate pier material used was 100 percent sand. The results showed that higher compaction leads to the highest ultimate bearing capacity for 100 percent sand piers, and that 100 percent gravel piers produced the highest overall ultimate bearing capacity.

Pitt, et al. (2003) discuss two separate series of tests conducted at different sites. Two single aggregate pier tests were conducted: one was installed by the vibroreplacement method, whereas the other was installed by the rammed method. During installation of the piers, K_0 stepped blade tests were performed. Since the subsurface is much better characterized for the rammed aggregate

pier test site, a direct comparison of the results is difficult. The native soil at the vibropier test site is characterized by 3 m of fill over soft, compressible, silt and clay. The native soil at the aggregate pier test subsite is characterized by 1 m of fill over lightly overconsolidated (OCR ~ 2), soft, compressible clay. The aggregate pier material used for both the vibro and the aggregate pier was uniform-graded gravel, the length and diameter were 5 m and 5.4 m and 0.91 m and 0.76 m for the stone column (vibropier) and aggregate pier, respectively. The aggregate pier performed unquestionably better than the stone column. The authors attribute this difference to lower lateral stress development in the stone column due to remolding of its surrounding soil based on the results of K_0 stepped blade tests.

Pitt et al. (2003), White and Hoevalcamp (2004), Wissmann et al. (2007), White et al. (2007), and Pham and White (2007) discuss a series of field load tests on single aggregate piers with different lengths of 2.29 m, 2.52 m and 4.6m. The native soil is characterized by about 1.2 m of fill, over soft, compressible normally consolidated clay. Pitt et al. (2003). The tests results show that the shortest aggregate pier tends to penetrate the soil below the base of the pier in a plunging (punching) manner for, with the tendency for plunging decreasing with increasing pier length. However, the sharp contrast between the 2.29 m and 2.52 m aggregate pier is confusing, particularly considering the comparison between the 2.52 m and 4.6 m aggregate pier. Pitt et al. (2003) attribute the difference in behavior to the presence of the stress cells within the instrument aggregate pier itself. It appears that the presence of the earth pressure cells, where the diameter of the cell equals the pier diameter, affected the load-displacement behavior of the pier.

Group of Aggregate Piers

Baumann and Bauer (1974) performed a full-scale test on a group of aggregate piers supported footing and compared the results with a footing supported by unreinforced soil. The test site is characterized by a superficial layer of sandy silt, 1 to 2 m thick, over silty, gravelly sand with a thickness of 0.8 to 1.7 m thick, over 40 m of varved, marine silty clay. The 1.35 m diameter footing was supported on three aggregate piers, 5.5m in length, compacted via vibration. This test setup produced an area replacement ratio of about 47 percent. The unreinforced soil shows a lightly strain hardening approach, whereas the reinforced soil appears to find a limiting bearing capacity. The settlement improvement factor (ratio of settlement of treated to untreated ground) is about 0.2 at a bearing pressure of 198.1 kPa, decrease to about 0.125 at a bearing pressure of 147.1 kPa.

Goughnour and Bayuk (1979b) conducted a full-scale field test on vibrated aggregate piers. The test site was characterized by 3.7 to 4.6 m of very soft to soft elastic silts and fat clays overlying loose to medium dense silty sands. The 6.3 m wide square footing used to apply load was constructed from 4 separate footings 3.05 m square, each separated by a 15 cm gap, to approximate a flexible boundary condition. The footing was supported on 17 aggregate piers, compacted via vibration, that averaged 1.1 m diameter and 6.3 m in length. A total load of 3.57 MN was placed over a 54-hr. time period. Observed settlement reached 79 mm at the center of the footing when all the load had been placed.

Lawton and Warner (2004) present a load test on a group of aggregate piers. The footing width was 1.98 m with no embedment. Aggregate piers were 2.44 m long and 0.61 m in diameter. The instrumentation used for the test consisted of nine total earth pressure cells (four in the matrix soil, five on the aggregate forming the pier) and one inclinometer casing installation located 30 cm

from the edge of the center of the footing. Additionally, four total earth pressure cells were placed within the aggregate piers at various depths. The authors suggest that failure occurred at a load of approximately 2610 kN and a displacement of 59 mm, with the failure mode by bulging of the aggregate piers. The total earth pressure cell observations show stress concentration ratios of approximately nine at small loads increasing with increasing up to the "failure" load, where a peak of 16 was observed; following peak, the stress concentration ratios decreased to near zero. Lawton and Warner (2004) suggest that the very small excess pore pressures developed during loads, less than the failure load, is due to the rapid completion of primary consolidation. However, it is more likely that pore pressures dissipated rapidly due to the relatively short drainage paths of the relatively thin interlayered cohesive soils coupled with the large coefficients of consolidation corresponding to recompression over the majority of applied loads.

Summary of Literature Review

Summary

The literature review presented above discussed: (1) various construction methods, (2) numerical modeling studies, and (3) full scale load test studies. Since the practicing geotechnical engineer relies heavily on field performance data, the literature review presented a review of a series of field load tests of aggregate pier improved ground in cohesive soils. The review showed a deficiency in the number of field load test data of end-bearing aggregate piers. Although the review presented provides a good starting point for use by engineers in practice, it is apparent that more information is required to supplement existing research.

Outstanding Problems and Issues

Based on the literature review, the following two concerns should be addressed in an effort to advance the state of the art in the design of aggregate piers supporting shallow foundations resting on fine grained clay type soil:

1. The lack of available field information regarding the performance of footings resting on aggregate pier reinforced clay soils, including but not limited to load displacement characteristics, stress concentration ratios, load-transfer, settlement and stress attenuation with depth, and lateral soil movement adjacent and below footings.

2. The lack of information comparing different construction variables, including aggregate gradation, aggregate compaction, pier lengths and end-bearing or floating conditions.

CHAPTER THREE: FIELD EXPERIMENT AND NUMERICAL MODELING OF A SINGLE AGGREGATE PIER

Introduction

The use of aggregate piers as a soil improvement method has been growing worldwide, which has made the understanding of the design and behavior of these elements more important than ever. Aggregate piers are considered floating foundation systems consisting of a stiff composite layer, typically to a minimum depth equal to the stress influence zone of the footing, used to reduce the applied pressure on the soil matrix and foundation settlement (Figure 1a). This composite layer by the aggregate piers and the soil around them is called the upper zone. The settlement of a foundation supported by aggregate piers is equal to the sum of the settlement contributions computed from the upper reinforced zone and lower unreinforced zone (Lawton and Fox, 1994; Lawton et al., 1994) (Figure 1a). The settlement within the upper zone is computed by treating the footing as a rigid element, the aggregate pier elements as stiff springs, and the soil around them as soft springs. Since the aggregate piers are stiffer than the surrounding soil, footing stresses concentrate to the piers, thereby reducing the applied stress on the soil. The compressibility of the upper zone is characterized by a modulus test that establishes an appropriate spring constant, or modulus, for the piers (Wissmann et al., 2007).

Figure 1b summarizes the typical installation process of aggregate piers. First, an auger drills a 60 to 90 cm diameter hole to a depth between 1.5 and 8.0 m from the ground surface. Open-graded base course material is placed at the bottom of the hole and forced into the soil using a high-energy impact tamper and a beveled tamper foot to form a bulb. The bottom bulb increases the effective design length of the aggregate pier by one pier diameter. The pier shaft is then

constructed by ramming thin lifts of around 0.3 m of material into the cavities. The aggregate materials are forced laterally into the sidewall of the excavated cavity, which increases the lateral stress in the surrounding soil, and the soil matrix is densified and prestressed (White et al., 2000; Handy, 2006; Wissmann et al., 2007).

The behavior of aggregate piers has been previously investigated using both experimental and numerical approaches (White et al., 2007; Pham and White, 2007; Handy and White, 2006a, b; Suleiman and White, 2006; Chen et al., 2009; Halabian et al., 2012a, b). Limited studies have considered the pier's installation effect, in which the lateral pressure effect on the soil matrix has been induced by cavity expansions along the shaft and at the bottom of the cavity caused by the ramming exerted by the hammer used to compact every lift of material (Pham and White, 2007; Chen et al., 2009; Halabian et al., 2012a; Pham, 2005). Stuedlein and Holtz (2012) and Wissmann et al. (2007) conducted a series of field experiments and investigated uncertainties associated with the effect of various installation techniques and materials which could lead to significant differences in observed performance. The observed responses indicated that aggregate piers with well-graded aggregate are stiffer than the uniform-graded aggregate piers. The results of their study also suggested that the capacity of a group of aggregate piers is the sum of all the individual's capacity. Halabian et al. (2012a) showed that the stress path for an adjacent soil element located at shallow depths of the pier in a group pier is affected by the pier installation. During pier installation, the radial normal stress increased beyond the vertical normal stress, and the shear stress also increased. At the end of the pier installation process, the stress state of the soil element approached the Rankine passive condition on the upper 25% of the pier's length. This is because the radial expansion is not constant along the Rammed Aggregate Pier (RAP) height. In the deeper

soil layers, as the overburden pressure increases, the radial expansion decreases so that a critical depth can be defined in which the radial expansion can be neglected. This critical depth increases with an increase in the aggregate pier diameter, friction angle, and soil matrix cohesion (Halabian and Shamsabadi, 2014).

This study uses two-dimensional (2D), nonlinear, finite difference analyses (FDA) and field load test data to investigate the effect of installation process and friction angle of aggregate materials on the load-displacement response of single aggregate piers (Halabian et al., 2012). The complete foundation system of a footing supported over an aggregate pier can adequately be analyzed by numerical simulation if the prescribed installation effects of piers are considered (Algin and Gumus, 2018). The load tests were conducted in a site consisting of undisturbed slopewash alluvial clayey and silty soils, lean clay, and gravels. The nonlinear analyses were first calibrated using the recorded load-displacement response of the aggregate piers. The calibrated model was then used to evaluate how various parameters, including the aggregate's friction angle and installation process (e.g., confinement), influence the load-displacement response of the aggregate piers.

Overview of Field Load Tests

The project consists of a new parking garage north of the Billings Clinic Hospital. The site was located on the south side of the lot between North 29th Street and North Broadway in Billings, Montana (Figure 2a). Six soil borings were completed in the area of the proposed garage. Figure 2b shows the variation of the standard penetration test (SPT) N value with depth for one of the borings in the site. The borings generally encountered a similar profile, consisting of about 2 to 3 m of undisturbed slopewash alluvial clayey and silty soils. Lean clay was then encountered to

depths of about 4 to 5 m. The borings terminated within a gravel layer at a depth of around 7 m. The water table was found at a depth of 6 m below the bottom of the aggregate pier.

The modulus load tests were performed on two 760 mm diameter piers. A detailed sketch and photo of the load test are shown in Figure 3. The aggregate piers extended to a depth of 4.5 m. The load tests were performed according to ASTM D1143 / D1143M – 20 and reached 150% of the pier design stress.

The pier was first built up to 0.6 m below the ground surface. A 25 mm thick round steel plate with the same diameter as the piers was placed on the top of the pier, leveled, and rammed the same way as the pier's lifts. A W-section pedestal with another 30 × 30 cm square steel plate of 25 mm thickness was then placed on the top of the steel plate. The hydraulic jack was aligned with the center of the square steel plate. The displacements of the top plate and tell-tale rebars coming from the bottom of the pier were recorded using two gauges to measure the pier's top displacement and two gauges to measure the pier's bottom displacement. According to the project specifications, the pier displacement had to be limited to 25.4 mm for a design stress of 800 kPa. To ensure that the indicated stress was reached, the hydraulic jack was calibrated to obtain a relationship between the pressure measured on the jack gauge and the actual force applied to the top of the pier.

Two different aggregate materials were used for construction of the aggregate piers, a base coarse material with a maximum particle size of 38 mm and a subbase coarse material with a maximum particle size of 75 mm. The grain size distribution (GSD) curves are shown in Figure 4. The aggregate materials are gap-graded with a fines content of less than 10%. Gap-graded aggregates contain aggregates retained on the No. 4 sieve, and particles passing a No. 40 sieve

(0.425 mm). The base material has a higher sand content (51%), while in the subbase coarse aggregate, intermediate sizes in the range of 0.85 to 4.75 mm are absent from the gradation curve. The compaction process of the aggregate piers was controlled using a dynamic penetration test (DPT) which was performed on the upper part or head of the aggregate pier at the end of the installation process. A minimum of 15 blows per 44.5 mm vertical penetration is specified (ASTM STP 399). For the base coarse aggregate, 45 blows were required to penetrate the probe 44.5 mm, while for the subbase material the number of blows per 44.5 mm was only 30. Based on Mohammadi et al. (2008) and based on the number of blow counts, a friction angles 52 and 48 degrees could be expected for the base and subbase coarse aggregates, respectively.

Figure 5 displays the load-displacement results of the pier obtained from the load tests on the two aggregate piers. The load-displacement curve for the subbase coarse material provides a stiffer initial response compared to the base coarse material, decaying with increasing applied bearing pressures beyond the design stress of 800 kPa. This behavior contrasts with that of the aggregate pier with base coarse material, which exhibits less rapid subgrade stiffness degradation. The load-displacement curve for the aggregate pier with base coarse material leads to smaller displacements with increasing applied loads. For the subbase material, the displacement was about 40% higher at 150% design stress compared to the pier with base coarse material. The measured displacement at 100% of the design stress was, however, similar (approximately 5 mm) for both piers, giving a pier reaction modulus of 160000 kN/m^3, which was significantly higher than the value of 55000 kN/m^3 used for the design. The difference in the load-displacement response between the two piers could be attributed to different aggregate materials, the stress dissipation

mechanism in the soil matrix around the pier and bulging in the upper part of the aggregate pier (Figure 8b).

Overview of the Numerical Simulations

Two-dimensional, nonlinear, axisymmetric analyses of the load tests were performed in the finite difference FLAC2D platform (Itasca, 2016) to evaluate the load-settlement behavior of the aggregate piers. The configuration of the baseline model is shown in Figure 6. The baseline model consisted of a 2.5-m-thick layer of lean clay with sand overlain by a 2.0-m-thick layer of lean clay. The aggregate pier was placed over a 5.5-m-thick layer of gravel. The bottom boundary of the model was fixed, and the lateral boundaries were fixed horizontally and left free vertically (Figure 6). The right lateral boundary was placed far enough (more than 4 diameters of the pier) to avoid any effect on the results (Halabian and Shamsabadi, 2014). The water table was below the bottom of the aggregate pier; therefore, the soil and aggregates were modeled with a Mohr–Coulomb model in an effective stress, uncoupled mode (no pore fluid). To account for the column installation effect, the lateral stress along the aggregate pier length and within the soil was increased. The stress along the upper 25% of the pier length was increased up to passive pressure, while for the lower 25% of the pier length, the stress was reduced to at rest pressure following the procedure proposed by Halabian and Shamsabadi (2014).

The soil and aggregate parameters, including unit weight (γ), friction angle (ϕ'), cohesion intercept (c') considered in these analyses are listed in Table 1. Model parameters of the soil layers were estimated based on the available correlations between the soil parameters and SPT N value (e.g., for cohesion: Jamiolkowski et al., 1985; for friction angle: Bjerrum and Simons, 1960). To obtain the friction angle for the upper two layers based on the Bjerrum and Simons (1960) chart,

liquid limits (LL) of 20 and 25 were considered for the Lean Clay with Sand Layer and the Lean Clay layer, respectively. The friction angles for the aggregate piers were estimated at 52 and 48 degrees for the base and subbase coarse materials, respectively (Pham, 2005; Geopier® Manual; and Mohammadi et al., 2008).

Numerical Results and Parametric Analyses

The simulated load-displacement response of the aggregate piers is shown in Figure 7, along with the field load test results for the aggregate pier built with the base (Figure 7a) and subbase (Figure 7b) materials. The computed load-displacement responses are consistent with the measured load-displacement results for both piers. The results indicated that a lower friction angle of 48 degrees gives similar results to the modulus test with the aggregate pier built with the subbase material. A lower friction angle was considered for the subbase material due to lower DPT blow counts per 44.5 mm (30 blow counts versus 45 blow counts for the piers built with base aggregate material).

Analyses were repeated with friction angles in the range of 48 to 52 degrees, while all other parameters were kept constant (Figure 8a). The effect of the aggregate pier friction angle on the load-displacement response of aggregate piers is shown in Figure 8a. The friction angle values are in the range of the typical friction angle recommended for aggregate piers by Fox and Cowell (1998). The results obtained from the field tests show a more linear behavior response for the pier built with the base material with a higher friction angle compared to the pier built with subbase material. This behavior is typically due to the stress dissipation mechanism in the soil matrix around the pier. For the aggregate pier built with a higher friction angle (base material), the load is transferred to a bigger part of the length of the pier. For an element built with a lower friction

angle, bulging of the upper part of the pier could occur; therefore, part of the settlement is due to bulging of the pier. Figure 8b shows the computed lateral displacement (bulging) at one meter below the ground surface for both base and subbase materials. Although bulging of the upper part of both piers started after the first load increment, it became more notable at stresses beyond 100% design stress, particularly for the subbase material.

Based on the results, it's shown that the 2D numerical analyses reasonably predict the aggregate pier load-deflection responses with the friction angle of the aggregate pier in the range of 48 degrees to 52 degrees. During the field test, it was found, based on the DPT testing blow count, that the fines content within the material used for the construction of the aggregate piers makes a difference in the compaction percentage. As a result, there is a higher densification and higher friction angle for the base material with lower fines content.

Note: E = elasticity modulus, c' = effective cohesion, ϕ' = effective friction angle, ν =Poisson's ratio

Layer	Depth (m)	Density γ (kg/m3)	E (kPa)	c' (kPa)	ϕ'	ν
Lean Clay with Sand	**0.0 – 2.5**	**1950**	**2.50E+4**	**2.0**	**32**	**0.40**
Lean Clay	**2.5 – 4.5**	**1760**	**1.50E+4**	**2.4**	**28**	**0.40**
Poorly Graded Gravel	**4.5 – 10.0**	**2000**	**3.00E+4**	**1.1**	**35**	**0.25**
Aggregate Pier	**0.0 – 4.5**	**2140**	**1.20E+6**	**1.0**	**52**	**0.20**

Table 1. Parameters for the soils and aggregate pier in the baseline model

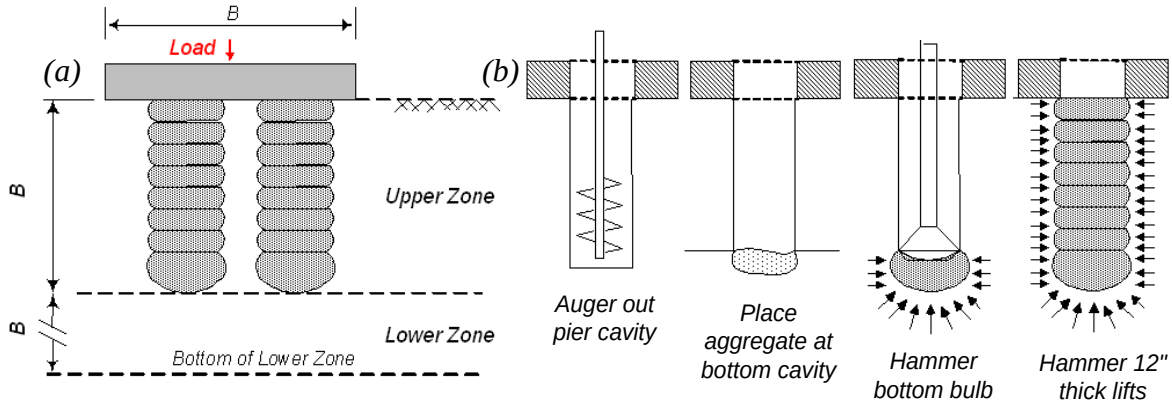

Figure 1. a) Schematic of upper and lower zones (Geopier® Manual), b) Aggregate pier construction process (Geopier® Manual)

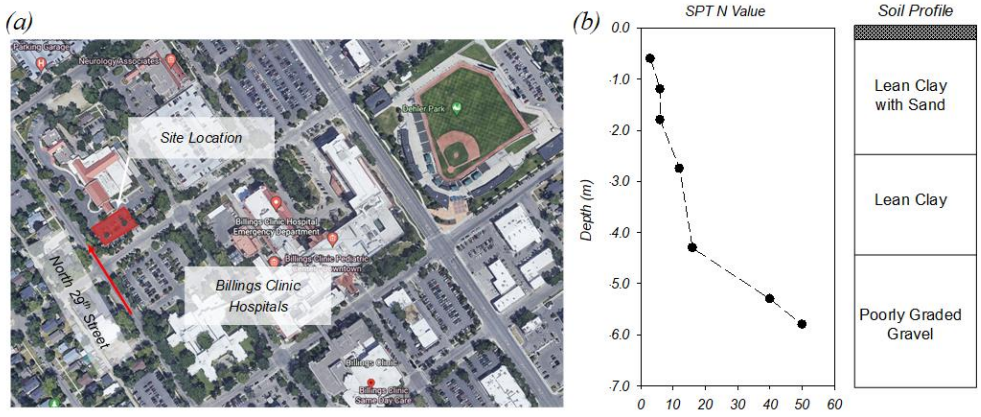

Figure 2. a) The location of the proposed garage (taken from Google Earth), b) Variation of SPT N values with depth

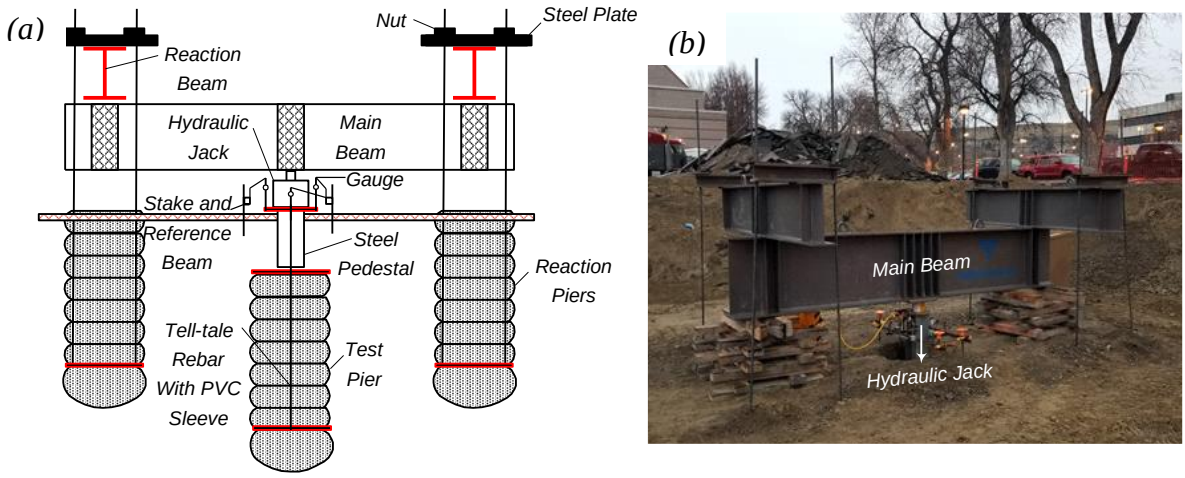

Figure 3. a) Sketch and b) Photo of the experimental load test setup

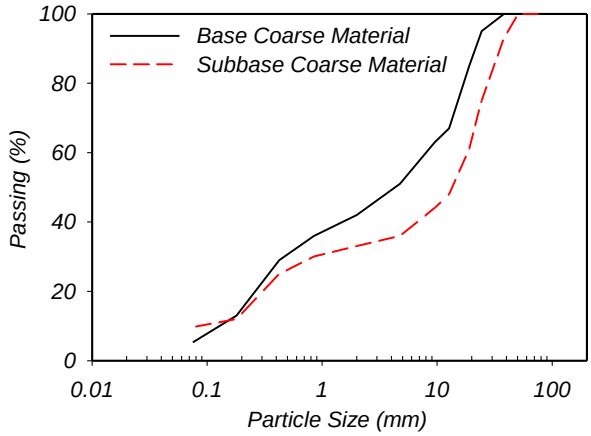

Figure 4. Grain size distribution of aggregate pier materials

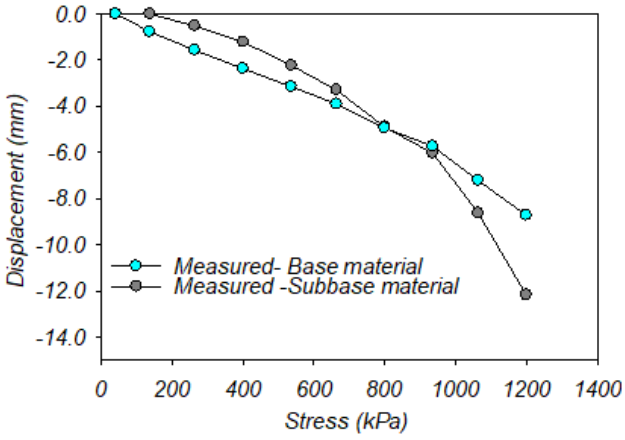

Figure 5. Load-deflection results obtained during field load tests

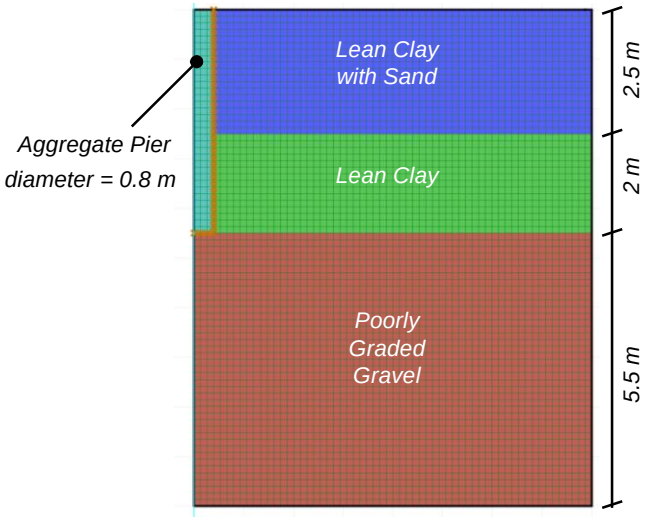

Figure 6. Numerical model configuration of the baseline model

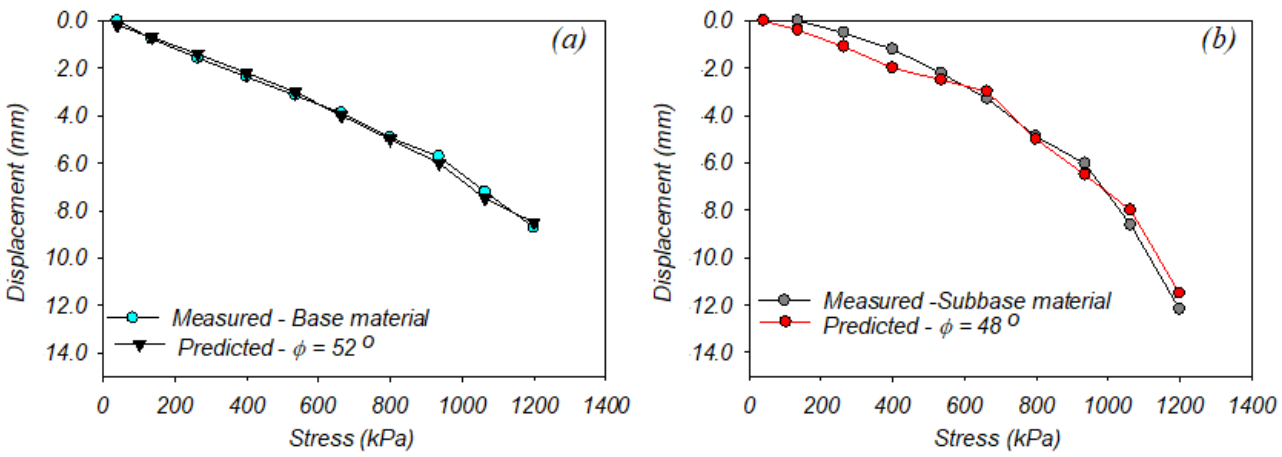

Figure 7. Deflection curves for site testing and numerical analysis

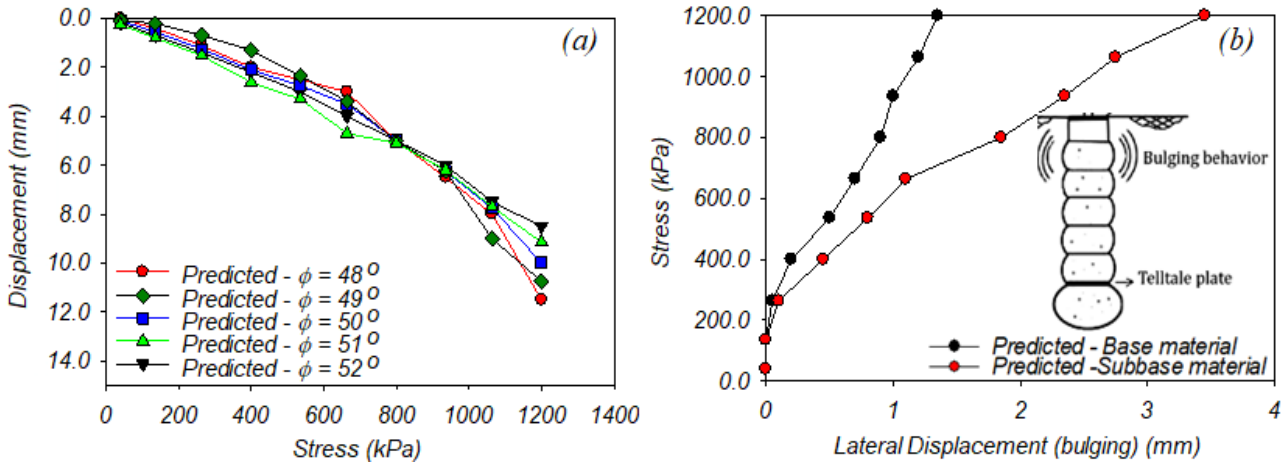

Figure 8. a) Effect of the aggregate friction angle on the load-displacement response of aggregate piers, b) Lateral displacement at 1m from ground surface

CHAPTER FOUR: STRESS TRANSFER MECHANISM AND CONSTRUCTION EFFECT OF END-BEARING AGGREGATE PIERS

Introduction

Aggregate piers can be used as an effective method for improving soft soil profiles for support of overlying structures (e.g., Lawton and Fox, 1994; Wissmann and Fox, 2000) or to reduce potential ground deformations under static or dynamic loading (e.g., Lawton et al., 1994; Wissmann et al., 2001) and mitigate liquefaction in sandy and silty soils (e.g., Wissmann et al., 2015). Due to their growing popularity as a ground improvement method, understanding the design and behavior of aggregate piers has become more important than ever. Design considerations include the ability of aggregate piers to withstand applied forces and stresses without excessive deformation (e.g., due to bulging near the surface or due to vertical displacement) and the ability of composite soil and aggregate pier systems to limit settlements or deformations to acceptable levels. The aggregate pier installation involves an auger drilling a 0.6m to 0.9m diameter hole and filling it with densely compacted aggregate materials. During the installation process, the aggregates in the cavity expand downward and laterally at the bottom of the cavity and laterally along the shaft, thereby prestressing and prestraining the matrix soil around the pier. The question is how the cavity expansion contributes to improved pier stiffness and how it impacts the mechanical properties of the surrounding matrix soils (Handy and White, 2006a, b; White and Suleiman, 2005; White et al., 2006).

Single aggregate piers may fail in one of the following possible failure modes depending on the length and strength properties of the in-situ soil (Figure 9): 1) bulging, which is limited to the upper portion, more prominent in stone columns longer than a critical length equal to four to

six times the diameter of the element (Hughes and Withers, 1974; Greenwood, 1970; Charles and Watts, 1983; Balaam and Booker, 1981; Black et al., 2007), and about three times the diameter of the element for aggregate piers (Wissmann et al., 2001); 2) general shear failure, which is likely to occur in short end-bearing aggregate piers (e.g., shorter than three times the diameter of the aggregate piers) with very high bearing pressure (Madhav and Vitkar, 1978; Geopier's Manual, 1998), and 3) punching failure, which is the prominent failure mode in short floating aggregate piers (Aboshi et al., 1979; Geopier's Manual, 1998). The interaction between aggregate piers in a group could restrain expansion and thus reduce bulging of neighboring piers (Wood et al., 2000). Bulging, shearing, and lateral deflection of aggregate piers is restrained in a 'conical' zone directly beneath the loaded area (e.g., footing) with zone depth depending on the area replacement ratio (Figure 10). The central aggregate pier deforms or bulges uniformly, whereas those at the edge of the group bulge away from neighboring piers (McKelvey et al., 2004; Babu and Shivashankar, 2012).

The behavior of aggregate piers under loading has been previously investigated, including contributions from the authors listed in Table 2. The focus of these studies has been on 1) load-deformation behavior (White et al., 2007; Wissmann et al., 2007); 2) installation techniques and materials (e.g., Stuedlein and Holtz, 2013); 3) interaction between piers in a group (e.g., White et al., 2007; Wissmann et al., 2007); and 4) installation effects (e.g., Handy and White, 2006; Gumus, 2018). Using a series of field experiments, Stuedlein and Holtz (2013) indicated that aggregate piers constructed using well-graded aggregate are stiffer than uniform-graded or open-graded aggregate piers. This observation is mainly due to the higher densification and higher friction angle reached during compaction. Wissmann et al. (2007) compared the results of a series of full-scale

load tests on floating single and group aggregate piers and suggested that the capacity of a group of aggregate piers is the sum of all the individual's capacities. Other studies, however, have suggested that load tests on isolated elements cannot be used to determine the capacity of a group and could overestimate the actual capacity of the group (Greenwood, 1991). Full-scale field tests have demonstrated that the performance of aggregate piers and stone columns under widespread loads depends on loading circumstances and pier-soil interaction, which cannot be simulated by load tests on single piers.

This paper presents results of a full-scale load test conducted on one trial footing supported by four aggregate piers and a load test on one isolated aggregate pier. Furthermore, the paper investigates stress-deflection behavior at different depths and the stress transfer mechanism within a single pier and group of piers. The main objectives are to investigate the stress transfer mechanism, the load-deformation behavior, and the construction effect generated by the construction of the aggregate piers. The results of the experiments are also compared with those in the literature to provide insights on the performance of aggregate piers with different configurations (single vs. group) and depths (floating vs end-bearing) in different soil profiles.

Site Geotechnical Investigation

The aggregate pier test site was located just outside the Marga Hosaeus Fitness Center on the Montana State University Campus, where an expansion of the building is underway. The subsurface investigation of the test site included: 1) a series of standard penetration tests (SPT) performed about 10 months before the load tests; 2) a series of cone penetration tests (CPT) on the exact location of the piers, performed one day prior to their construction; and 3) a series of CPTs conducted after the aggregate pier construction to evaluate the aggregate pier installation effects

on the in-site soil strength properties. The locations of the CPT before and after the installation of the aggregate piers are shown in Figures 12 and 13. The subsurface profile is shown in Figure 11. The ground water table was about 5 to 6 m below the ground surface. The average elastic modulus value for the soil surrounding the piers was approximately 30 MPa. Estimated values for the coefficient of lateral earth pressure, K_o, were 0.6 for the sandy silt and clayey silt and 0.5 for the silty clay. The data interpretation procedures and correlations used are fully described in Kulhawy and Mayne (1990) and Hoevelkamp (2002). Laboratory index tests conducted in this study included soil classification, water content, and one-dimensional consolidation test. In-situ moisture content was about 20%.

An Overview of the Experimental Program

Two load tests were performed on sacrifice aggregate piers with a length of 4.3m and a diameter of 0.76 m. The site soil profile consists of soft to medium stiff layers of sandy silt and clayey silt overlain by a 2-m-thick, softer silty clay layer. Below this, at about 5.5 m, sandy gravel and weathered bedrock were found (Figure 11). The aggregate piers were constructed using 38.1 mm of crushed base classified as poorly graded gravel (GP) (C_u=48.82; C_c=0.49) with 4.9% by weight passing the No. 200 sieve and unit Weight, γ, of 21 kN/m^3. The compaction process of the aggregate piers was controlled using a dynamic penetration test (DPT) performed on the upper layer or head of the aggregate pier at the end of the installation process. For the base aggregate material used, 45 blows were required to penetrate the probe 44.5 mm, which meets the minimum value of 15 blows per 44.5 mm vertical penetration specified by the American Society for Testing and Materials (ASTM STP 399). Based on Mohammadi et al. (2008) and based on the number of blow counts, a friction angle of 52 degrees could be expected.

Prior to the construction of aggregate piers, inclinometer casings were installed at the locations indicated in Figures 12 and 13 (0.3 m, 0.9 m, and 1.5 m from the edge of the instrumented piers). Pier construction commenced with drilling the instrumented pier of the footing test to the indicated depth and backfilling in compacted lifts of base coarse aggregate. During the installation of the aggregate pier, four tell-tales and load cells were placed at the elevations shown in Figure 12. After the installation of the instrumented pier, the other three piers were installed, and the footing was constructed. After construction of the concrete footing, the same drilling and backfilling process was followed for the instrumented single pier test. Additional CPT tests were performed after the single and group pier installation to investigate the effect of pier installation on strength properties of in-situ soil.

The first load test was a full-scale load test using a square 2.1 meters concrete footing supported by four aggregate piers, from now on called F1 test (Figure 12). The footing was loaded to 1058.4 kN, corresponding to a bearing pressure of about 240 kPa. Load increments were held until the rate of movement was less than 0.25 mm per 15 min (Stark and Yacyshyn, 1991) or 64 min, whichever occurred first. The maximum applied load was defined based on the recommended design maximum allowable bearing pressure for this type and consistency of soil (Geopier's Manual). For test F1, first a compression stress of 240 kPa was reached, then it was diminished to 5% of the applied pressure, and then the stress was increased again until the maximum compression pressure reached 360 kPa. The second test was conducted on a single pier, from now on called P1 test (Figure 13). P1 was loaded to 365 kN, corresponding to a bearing pressure of about 800 kPa. The maximum applied load was defined based on the recommended maximum pier pressure for this type and consistency of soil (Geopier's Manual). For P1, first a compression stress of 800 kPa

was reached, then the pressure was diminished to 5% of the applied pressure, and then the load was increased again to a maximum compression pressure of 1600 kPa. A 2500 kN hydraulic jack and beams capable of withstanding the load were used (Figures 12 and 13). As reaction elements, four round 115mm diameter helical piles were installed down to the weathered bedrock depth. A 25.4mm thick and 0.8m diameter steel plate was used between the bottom of the hydraulic jack and the top of the concrete footing to distribute the load on a larger area of the footing. In both cases, total load was divided into ten equal increments and each one was maintained for no less than 15 minutes. The load cells were programmed to take a reading every minute during the entire duration of the test. A vertical deformation reading was taken right after every increment of the load and before the next increment of the load. The same reading schedule was used for the unloading stage of the tests.

The P1 test was instrumented with three load cells. The upper load cell was located at the top of the aggregate pier at 0.3 m from the bottom of the upper steel plate, the bottom load cell was at 0.3 m from the bottom of the pier (above the first layer of compacted material or bottom bulb), and one load cell in the center of the pier at 2.1m measured from the bottom of the upper steel plate. To obtain the vertical deformation and the stress at the same depths, tell-tale reference plates were used at the same location of the load cells. For the F1 test, only one of the aggregate piers was instrumented. Instrumentation included four load cells and four tell-tale reference plates located at different locations through the depth of the aggregate pier. The upper load cell was located at the top of the pier at 0.3 m from the bottom of the footing, the bottom load cell was at 0.3 m from the bottom of the pier (above the first layer of compacted material or bottom bulb). The other two load cells were located in between the length of the pier at 1.5 m and 2.7m measured

from the bottom of the footing. Tell-tale reference plates were used to record the vertical deformation at the same location of the load cells. Figure 14 shows the detail of the tell-tale steel plates that were used at each location of the load cells.

Test Results

The bearing pressure-displacement (q-δ) behavior of the two full-scale in-situ load tests, one on a single aggregate pier and one on a footing supported by a group of four aggregate piers, are presented to illustrate the load distribution along the length of the piers and examine the effect of aggregate pier installation on in-situ soil strength properties. The results include (1) q-δ behavior of isolated and group aggregate piers, (2) vertical stress distributions, (3) effect of in-situ properties on response of aggregate piers, (4) a comparison of q-δ behavior of aggregate piers with other studies, and (5) stress distributions along the depth of aggregate piers.

Bearing Pressure Displacement (q-δ) Behavior of Single and Group Aggregate Piers

The *q-δ* behavior of the P1 test alongside the F1 test are shown in Figure 15. Each figure displays the pressure-displacement curves from different depths along the isolated P1 (Figure 15a) and group F1 (Figure 15b) aggregate piers. The load-settlement responses of both tests are quite linear, where the single pier exhibits greater final vertical displacements than those of the group. The final applied stress concentrated on top of the piers was higher for the single pier compared to the piers supporting the concrete footing. The single aggregate pier experiences, on average, approximately 9 mm of displacement at the top for the final load increment, while the group aggregate pier exhibits a displacement of 5 mm at the top for the final load increment. The total

settlement for both cases is less than the typical design value of 25.4 mm, meaning that both single and group aggregate piers were able to support more load and did not reach failure, based on displacement criteria, at the maximum load applied.

The load-settlement curves at different depths along the aggregate pier are used to understand the prominent mode of deformation of the aggregate piers. As mentioned earlier, two common modes of deformation of piers installed in homogeneous soft to medium soil are bulging and punching (or tip movement). Bulging occurs when the difference between the top of the pier and the tell-tale settlements increases with increasing load (Pham et al., 2005). On the contrary, tip movement can be recognized when tell-tale movement follows the top-of-pier movement path and there is a point of increasing curvature on the tell-tale load-settlement curve with increasing load (Pham et al., 2005). Based on the measured displacements at different locations using the tell-tale reference plates, the dominant deformation mode for both F1 and P1 tests is bulging. In both instrumented aggregate piers, bulging started forming in the upper portion of the piers but based on the shape of the plots no failure was observed. According to Wissmann (1999), the bulging depth for an isolated pier can be approximated as:

$$z_b = z_o + 0.5D\ tan(45 + \emptyset'/2) \qquad \text{Eq. (1)}$$

where Z_b= bulging depth measured from grade; Z_o = depth to the bottom of the pier cap; D = diameter of the pier shaft; and $\emptyset'$ = effective stress friction angle of the pier material. Equation 1 gives a value of 1.70 m for both P1 and F1 cases (measured from ground elevation) which agrees with the bulging depth of about 1.5 m for the footing test (between 0.9 m and 2.1 m measured from ground elevation) but overestimates the bulging depth of the single pier. For the P1 test, bulging occurred between the top plate located at the head of the pier at elevation -0.6m and the tell-tale

located at elevation -0.9 m (Figure 13). Below this elevation, the bulging was negligible. For the F1 test, bulging occurred between the bottom of the footing at elevation -0.6m and the tell-tale located 1.5m below the bottom of footing at elevation -2.1 m (Figure 12). Below the -2.1m tell-tale, the bulging is negligible. The results suggested that bulging occurs at a depth of about 0.5 times the width of the footing, and the bulging depth changes for the single pier test and footing pier test.

Vertical Stress Distributions

The vertical stress distributions measured from the load cells placed within the shafts of the instrumented piers are presented in Figure 19. The vertical stress increase at a given load cell is calculated as the difference between the vertical stress measured at every load increment and the vertical stress measured immediately after the construction of the aggregate piers. The distributions of vertical stress increase show a linear increment at all load cell locations at every load increment. As shown in Figure 19a, for P1, at the maximum stress applied, the stress at 1.8 m from the top of the pier is about 20% of the stress at the top of the pier, and the stress at the bottom of the pier is about 10% of the stress at the top of the pier. In the case of the F1 test (Figure 19b), at the maximum stress applied, the stress at 1.5 m from the top of the pier is about 25% of the stress on the top of the pier and stress at the bottom is about 15% of the stress on the top. There is a difference in the residual stress at the bottom of the aggregate pier, with a larger residual stress for the footing test. The difference was expected considering the deeper bulb of pressure caused by the wider concrete footing. The stress dissipates rapidly with depth within the first two meters of the pier shaft, followed by smaller dissipation rates below the top two meters, indicating that the stress dissipates at a higher rate within the bulging depth.

Effect of In-Situ Properties on Response of Aggregate Piers

To investigate the effect of in-situ soil properties on q-δ behavior of aggregate piers, the results of this study were compared with those obtained by White et al. (2007) and Wissmann et al. (2007). Figure 17 compares the subsurface profiles and penetration test results. The CPT tests conducted in this study display a higher shear strength in comparison to those of White et al. (2007) and Wissmann et al. (2007). For both White et al. (2007) and Wissmann et al. (2007), the undrained shear resistance of the soil surrounding the piers was about 30 kPa, while for this study the average undrained shear resistance was about 150 kPa (see Robertson and Campanella, 1986). For both White et al. (2007) and Wissmann et al. (2007), the bearing layer was at about 14m from ground elevation, while in this study, the bearing layer was at about 5.5m. Considering the total length of the piers of about five meters, for the first two studies the piers behave as floating elements while for this study, the piers were supported on a bearing layer. According to the design methodology, the upper zone is the drill depth plus one diameter of the pier, in this case the upper zone is equal to 5.7 m from ground elevation.

Comparison of q-δ Behavior of Aggregate Piers

Figure 16 compares the load-settlement response of the F1 and P1 load tests of this study with those obtained by White et al. (2007) and Wissmann et al. (2007). The results include the response of the top and bottom of the piers. The load-settlement response of White et al. (2007) and Wissmann et al. (2007) show a bulging failure mechanism. As mentioned in previous sections, the piers of this study did not appear to have failed; however, the load-settlement curve in Figure 15 shows that settlement difference between the top of the pier and bottom of the pier increased

with every load increment, suggesting that bulging initiated from early stages of the loading. The measured values for this study show a smaller settlement for similar load applied for both single and footing tests. As shown in Figure 16.a, for a load of 1600 kN applied to the concrete footing, the top settlement measured by White et al. (2007) is about 6 times higher than the settlement measured in this study. Wissmann et al. (2007) show a similar final settlement to White et al. (2007) but at a lower load of about 1100 kN. The difference between the results could be due to higher strength properties of the in-situ soil surrounding the aggregate piers. The settlement at the bottom for all the studies is small, meaning that the stress is being dissipated within pier depth. Even if the pier is acting as a floating or end bearing element, they both can dissipate the stress coming from the footing effectively; the difference is that the floating piers develop slightly more bottom displacement to dissipate the stress.

If we compare the results from White et al. (2007) with the results obtained in this study, an important observation is that in both cases, the settlement at the bottom is small, so a big part of the total settlement is due to lateral displacement or bulging of the pier and is not due entirely to vertical displacement. The results suggest that when defining the capacity and expected settlement of the aggregate piers during the design of aggregate piers supporting isolated footings, the strength properties of the surrounding soil are more important than reaching a bearing layer, as long as the length of the pier is enough to dissipate the stress applied by the footing.

Furthermore, the results suggest that the aggregate pier configuration (floating vs end-bearing), in this scenario, has negligible effects on the behavior of the aggregate piers. When the pier is long enough to dissipate the stress, the lower zone is close to zero, meaning that there is no stress transfer below the length of the pier.

Stress Distributions along the Depth of Aggregate Piers

Figure 20a shows the vertical stress distribution at different load increments along the instrumented pier in the F1 Test. Figure 20b presents a comparison between the results obtained in this study and those of White et al. (2007). In this case, the pier length measured by White et al. (2007) was 2.97 meters. Figure 20b shows that the stress at the top of the aggregate piers is similar for similar applied load to the footing in both studies, but when the maximum load was applied, stress was about 150% higher for this study than the stress measured by White et al. (2007). The difference between the results is more pronounced in the measured stress at the bottom of the aggregate piers. The results of this study recorded that the stress at the bottom of the pier is about 15% of the stress measured at the location of the upper load cell, while in White et al. (2007), the stress in the bottom was about 60% of the stress measured at the location of the top load cell. The difference between the results can be attributed to: 1) the difference in length and aggregate pier end-bearing versus floating conditions and 2) the difference in strength properties of the surrounding soil.

As discussed before, the length of the aggregate pier in White et al. (2007) was 2.97 meters and the bottom load cell was located 1.8m from the ground surface. Based on the results of this study, the stress at a similar depth is about 25% of the stress at the top load cell compared to 60% of White et al. (2007). Due to its shorter length, floating condition, and softer in-situ soil, in the shorter pier of White et al. (2007), two different failure modes were involved: displacement of the whole element (e.g., punching) and bulging. The longer piers dissipate the stress better than short piers because they have a longer shaft to transfer the load to the surrounding soil. Another important aspect is that there is a difference in the percentage of stress dissipation at similar

elevations. At about 2.5 times the diameter of the pier, the stress dissipation within the piers for this study is about 75% of the calculated stress from the applied load at the top, while for White et al. (2007) it is only about 40%. The more rigid native surrounding soil helps create a more rigid pier that appears to be more effective in dissipating stress and less prone to large bulging or lateral displacements.

Group Effect

The group effect has been studied before, but the results from previous studies are not conclusive. Typically, the group effect is measured by comparing the settlement of a single pier and the settlement of a group of piers at similar pressure or load. According to Pham (2005), the group efficiency is about 1, meaning that the settlement of a single pier is the same as the settlement of the piers under a footing when they are under the same applied stress. Barksdale and Bachus (1983) reported similar results for stone columns. On the other hand, Lawton and Warner (2004) found that as the applied stress on top of the pier increases, the settlement of the single pier is smaller than the settlement of the group of piers for similar magnitudes of pressure on top of the pier. They defined this as a "negative" group effect. Greenwood (1991) studied the group effect of stone columns supporting liquid gas sphere tanks.; in his research it is mentioned that the capacity of the stone columns was confirmed by testing a single element and similar behavior was assumed for the group of stone columns. Later they found that this assumption caused failure on the foundations of the liquid natural gas spheres. The field full-scale experiments done by Greenwood (1991) demonstrates that the changing ratio of stresses on columns and intervening soil as the load is applied confirms load sharing between columns and soil. The variation in relative stiffness of

column and soil determines whether the response is mainly of reinforcing or load transfer to lower strata.

Loading a single pier vs loading a group of piers under a footing changes the interaction and stress dissipation between the aggregate pier and the surrounding soil. When a single pier is loaded, the stress transfer mechanism is similar to a pile; part of the stress is transferred by friction between the aggregate pier and the surrounding soil (Pham, 2005), and a small amount of stress is transferred by the tip of the pier, especially if there is a bearing layer supporting the pier. When a group of piers under a footing are loaded, there is load sharing between the aggregate piers and the surrounding soil (Greenwood, 1991). In this case the load is supported by the composite system formed by the piers and the surrounding soil where both support part of the load that is being applied. The aggregate piers support the major part of the load due to the stress concentration, but there is a residual stress that is supported by the surrounding soil. The stress concentration and residual stress depend on the relative stiffness between the piers and soil matrix. This interaction cannot be measured by a single pier test.

Group Efficiency

Group efficiency can be determined based on 1) pier capacity, defined as the point of increasing curvature on the load-settlement curve (White et al., 2007), or 2) settlement at the top of the pier (White et al., 2007). As mentioned above, the load-deformation curves were a straight line during the entire duration of the test, with no increasing curvature on the load-settlement curve (Figure 15). Alternatively, the group efficiency can be expressed in terms of settlement (White et al., 2007) and can be obtained as the settlement at the top of the single pier test divided by the settlement at the top of the instrumented pier from the group test. Figure 18 shows a plot of the

group efficiency for similarly applied compressive stress on top of the pier. The results show that the group efficiency decreases as the stress becomes higher. For a compressive load of about 50 kN, the group efficiency is about 1.4. For a compressive load of about 350 kN, the group efficiency is slightly lower than 1.0. As the stress gets higher, the group efficiency gets smaller, suggesting that the settlement of the footing is higher than the settlement of the single pier for equal measured stress within the piers.

A comparison between the results from White et al. (2007) and this study shows some differences. According to White et al. (2007), the group efficiency is about one, while in this study it was found that the group efficiency is slightly higher than one, but it tends to decrease as the load or stress on the aggregate piers gets higher. The negative group effect found here is attributed to the failure mechanism and the fact that for the P1 test, all the load is being supported by the pier, meaning that all the settlement is due only to the settlement of the pier. In the case of the F1 test, there is a stress concentration at the piers, but part of the load is supported by the less rigid surrounding soil. If the soil stress increases, it could cause a larger settlement at the soil. The interaction and load sharing between piers and soil would be reflected in the overall settlement reading, causing a larger settlement in the pier-soil matrix.

Stress Concentration

The computed stress ratios between the footing, aggregate piers, and the soil underneath the footing are presented in Figure 19. Figure 19a present the ratio of the computed stress applied to the footing, q_T, to the computed stress carried by the pier, q_p, at the depth of 0.3 m below the footing, while in Figure 19b, the ratio of the computed stress carried by the pier at the depth of 0.3 m, q_p, to the stress carried by the soil underneath the footing, q_m, is presented. q_T is the applied

load on the footing divided by the footing area and q_p is the measured load in the load cell located at 0.3 m below the ground surface divided by the pier cross-sectional area. As shown in these figures, the stress transferred to the aggregate pier is more than two times greater than the computed stress applied to the footing (q_p = 510 kPa versus q_T = 240 kPa), whereas the applied stress on the enclosed soil is about 1/10th of the load carried by the aggregate piers (q_p = 510 kPa versus q_m = 47 kPa). The concentration of stress on the aggregate pier is attributed to the greater stiffness of the aggregate piers compared to the stiffness of the surrounding soil. As discussed in previous sections, the governing failure mechanism of aggregate piers is bulging, therefore the stiffness ratio between the aggregate pier and the soil depends on the stiffness of the soil surrounding the aggregate piers. For soils with higher initial stiffness, the expected stiffness of the aggregate pier will be higher, however, the ratio between the two could be constant. To investigate the effect of soil strength properties and stiffness on the stress transfer between the aggregate pier and surrounding soil, the results of this study with the soil surrounding the aggregate pier having S_u = 150 kPa are compared with those reported by White et al. (2007) with the soil surrounding the aggregate pier having S_u = 30 kPa. As shown in Figure 20b, the calculated stress at the location of the upper load cell in White et al. (2007) (depth of -0.3 m from the ground surface) was about 1.7 times greater than the calculated stress applied on the footing, while for this study the ratio of q_p/q_T was about 2.0. The stiffness ratio between pier and soil is assumed to be close to be constant except for really stiff or really hard soils where this value tends to decrease (Geopier® Manual). Typical stiffness ratio values used on aggregate pier design range from 7 to 10 for soils with SPT N values between 1 to about 12 (Geopier® Manual) which can explain the similar stress concentration values measured by this study and by White et al. (2007).

Stress Concentration Ratio. The stress concentration ratio is defined as how much stress is supported by the pier in comparison to the stress that is being supported by the native surrounding soil. Figure 20a shows that for the F1 test, the calculated stress at the top load cell location was 510 kPa for the maximum load applied to the footing, which corresponds to a vertical load of 234.6 kN per pier (938.4 kN for all piers). The maximum vertical force applied at the top of the footing was 1058.4 kN, so the remaining load supported by the surrounding soil was only 120 kN. This represents a stress of 46.41 kPa applied to the surrounding soil. Comparing the stress on the piers against the stress on the surrounding soil, there is a stress concentration ratio of about 11 at the design stress applied on top of the footing. Figure 22b shows how the stress concentration ratio (stress at pier divided by stress at soil) varies with increasing stress applied to the footing. The calculated stress concentration ratio ranges between 10 to 15, with an average value of 11 for the whole duration of the test. Measurements by Lawton and Warner (2004) for a group of nine aggregate piers installed in a relatively stiff clay indicated that the stress concentration ratio could be as high as 16. Typical values of stress concentration ratio for stone columns range from 2 to 5 (Goughnour et al., 1979; Barksdale and Bachus, 1983).

It is possible to compare the measured results obtained here with the results obtained using static equilibrium. For static equilibrium to occur, stresses within the footing must redistribute and concentrate on the aggregate piers according to the following equations (Geopier® Manual):

$$q_m = \frac{q}{R_a(R_s-1)+1} \qquad \text{Eq. (2)}$$

$$q_p = q_m R_s \qquad \text{Eq. (3)}$$

where q is footing design bearing pressure, q_p is bearing stress on the pier element, q_m is bearing stress on matrix soil, R_s is modulus stiffness ratio defined by the modulus of a pier element (k_p)

divided by the matrix soil modulus (k_m), and R_a is the area ratio defined as pier element(s) area (A_p) divided by the total footing area (A).

Once the stresses on the pier elements and the matrix soil are calculated, the settlement of the upper zone (S_{uz}) can be calculated as follows (Geopier® Manual):

$$S_{uz} = \frac{q_p}{k_p} \qquad \text{Eq. (4)}$$

where k_p is the pier modulus or pier spring constant obtained from a single pier load test (Wissmann et al., 2007).

As shown in Figure 22, having a rigid concrete footing causes the stress to redistribute and concentrate to the aggregate piers. Thus, it is possible to apply equations 2 and 3. The results obtained by these equations are as follows:

$$q_m = \frac{q}{R_a(R_s - 1) + 1} = \frac{240kPa}{0.414(10 - 1) + 1} = 50.78\ KPa, \quad (from\ Eq.\ 2)$$

$$q_p = 50.78\ KPa \times 10 = 507.83\ KPa, \quad (from\ Eq.\ 3)$$

According to Geopier's manual, typically a modulus stiffness ratio, R_s, of 10 is a good starting point. The results obtained above show almost identical results from what was measured on site.

Pier Stiffness

The stiffness of aggregate piers, k_p, can be calculated based on spring theory as follows (Geopier® Manual):

$$k_p = \frac{q_p}{s_p} \qquad \text{Eq. (4)}$$

where S_p is the settlement of the aggregate pier and q_p is the stress concentrated on top of each individual pier. k_p can be calculated using the spring analogy and Equations 1 and 2 (Lawton and

Fox, 1994). In design practice, the stiffness of an individual pier in a pier group is assumed to be equal to that of an isolated pier of the same length and diameter (White et al., 2007; Wissmann et al., 2007).

Figure 23 shows the pier stiffness ratio, defined as the stiffness of a single pier divided by the stiffness of the instrumented pier of the pier group, at three different locations: the top of the pier, 0.3m below the bottom of the footing, and 2.0 m below the bottom of the footing. Stiffness was found from the load cells and the deflection readings at the same depths. The line representing a stiffness ratio of 1 (e.g., the stiffness of an individual pier in a pier group is assumed to be equal to that of an isolated pier) is also shown for comparison. On the top of the pier, the stiffness ratio varies from a value of about 0.7 to 1.0, suggesting that the stiffness of the single pier is comparable to that of a pier in a pier group. At 0.3 m below the bottom of the footing, however, the stiffness ratio presents an average value of 4, suggesting that the stiffness of the single pier is significantly higher than the stiffness of a pier in a pier group. For the single pier, bulging happens between the top of the pier and the load cell located at 0.3m, while for the footing test, bulging of the piers happens at a depth of about 1.5m (Figure 15). The stiffness ratio at 0.3 m from the top of the single pier doesn't account for bulging because bulging happens above this elevation. However, for the pier group, bulging is still considered because bulging happens below this elevation. The stiffness ratio at 2.0 m below the bottom of the footing presents an average value of 0.3, meaning that the stiffness of the single pier will be lower compared to the stiffness of the piers supporting the footing. On average, it can be concluded that the total stiffness ratio at the surface is around one suggesting that the stiffness measured on a single pier test (in the appropriate location) could be

considered as the representative of the stiffness for the group of piers supporting an isolated concrete footing.

The results of these experiments are consistent with those reported in the literature for aggregate piers in dry and unsaturated conditions (e.g., White et al., 2007; Wissmann et al., 2007). For saturated condition, however, data from a series of field experiments on isolated and group stone columns and case history data from a group of stone columns supporting a gas tank with an 18 m radius showed that testing single elements and assuming similar behavior for the group of elements could overestimate the capacity of the group (Greenwood, 1991). The stress increase due to loading on a pier group can increase the pore water pressure in the soil surrounding aggregate piers. The increase in pore water pressure results in a reduction of radial constraint and loss of strength of the surrounding soil, and thus a reduction in pier stiffness due to bulging. Reduction in pier stiffness results in an increase in the load carried by the soil, leading to excessive settlement and failure of the structure.

Construction Effect

Aggregate pier installation involves an auger drilling a 60 to 90 cm diameter hole and replacing it with densely compacted aggregate materials. Numerical simulations using finite element analysis (e.g., Pham and White, 2007), hybrid finite difference-DEM modeling (e.g., Halabian and Shamsabadi, 2014), and field experiments using a K_o stepped blade (Handy and White, 2006) have suggested that the performance of aggregate piers could be influenced by the construction method (Stuedlein and Holtz, 2012; 2013). Drainage and compaction occurring during ramming of succeeding layers of the pier develop a distribution of radial effective stresses around the aggregate pier (e.g., Halabian and Shamsabadi, 2014). The radial normal stress on the

soil element around the aggregate pier could exceed the vertical normal stress, which results in a radial expansion in the soil surrounding the aggregate pier (e.g., Halabian and Shamsabadi, 2014; Handy and White, 2006). The increase in lateral pressure could improve the coefficient of lateral pressure up to a passive value for the upper 25 % of the pier's length (Halabian and Shamsabadi, 2014). Since stresses in the soil matrix cannot exceed the passive limit if no failure happens, the stresses around the pier will not exceed this limit (Halabian and Shamsabadi, 2014). The lateral stresses induced during the aggregate pier construction decrease the expected lateral displacement or bulging once the pier is loaded. The radial expansion is not uniform along the aggregate pier's height, it decreases with depth due to higher overburden pressure. The radial expansion can be neglected below a critical depth. This critical depth increases with an increase in the aggregate pier diameter, friction angle, and soil matrix cohesion.

To further investigate the installation effect on soil around the aggregate piers, a series of Cone Penetration Tests (CPTs) were performed before and after installation of aggregate piers (Figure 26 and figure 27). Lateral displacement around the aggregate piers was monitored using inclinometers installed around the piers before and after their construction. The inclinometer casings were installed at 0.3 m (I1 in F1 and I4 in P1), 0.9 m (I2 in F1 and I5 in P1), and 1.5 m (I3 in F1 and I6 in P1) from the edge of the aggregate piers in F1 (Figure 12) and P1 tests (Figure 13). The results were compared with the initial inclinometer measurements recorded prior to the pier installation. Figure 24 shows profiles of soil lateral movements due to pier installation. The lateral displacement profile demonstrates a non-uniform distribution along the aggregate pier height, with larger displacement at the top compared to the bottom of the pier. This difference is mainly due to higher confining stress. For inclinometer I4 located at 0.3 m from the edge of the pier, the lateral

displacement at the top of the pier was 2.5 mm; for the bottom of the pier, it was slightly lower than 1.0 mm. For the inclinometers I5 and I6 located at 0.9 m and 1.5 m, the deformation profile was more uniform with lateral deformations of less than 1.0 mm and 0.5 mm at the top and bottom of the pier, respectively. Compared to the single aggregate pair, the soil surrounding the group aggregate pier (Figure 24) experienced a larger and more uniform displacement along the aggregate pier length during installation. For the inclinometer I1, located at 0.3m from the edge of the pier, the lateral displacement at the top and bottom of the pier was 3.2 mm and 2.0 mm, respectively, which was about 150% higher than what measured in the P1 test. For the inclinometers I2 and I3 located at 0.9 m and 1.5 m, the lateral displacement at the top of the pier was only 1.5 mm and 1.3 mm, respectively. Lateral displacements at the bottom (~ 0.5 mm for I2 and 0.2 mm for I3) were negligible.

Figures 26 and 27 show the Cone Penetration Test (CPT) results obtained before and after construction of the aggregate piers for the P1 and F1 tests, respectively. For the P1 test, CPT5 was performed before the installation of the pier and CPT6 and CPT7 were performed after the installation of the pier. For the F1 test, CPT1 was performed before the installation of the piers, and CPT2, CPT3 and CPT4 were performed after the installation of the piers. All post-installation CPT tests were located 0.3 m from the edge of the pier. As shown in Figure 24, although the soil surrounding the aggregate pier experienced lateral deformation during the installation of the aggregate piers, its strength properties are not significantly influenced by the construction of the aggregate piers. The CPT results suggest that a maximum lateral displacement of 3.0 mm appears to be insufficient to fully mobilize the passive condition around the aggregate pier. The results could be affected by the type of soil and initial mechanical properties of the soil matrix. As shown

by White et al (2007), a softer fine-grained material, with lower elastic modulus, around the pier could lead to larger lateral displacements of the soil matrix (Figure 25).

The statistical significance of the installation effects on the strength properties of surrounding soil were assessed using ANOVA analysis. To determine the statistical significance of the control variables, the ANOVA was performed as a single factor ANOVA analysis because only one variable is being analyzed (i.e., tip resistance).The analysis is focused on the tip resistance because it is the variable used to determine the shear strength properties of the soil, friction angle (Robertson and Campanella, 1983), in-situ lateral stress coefficient (Kulhawy and Mayne, 1990), and cohesion or undrained shear strength (Baligh et al., 1980; Schmertmann 1975). In the analysis, the F value corresponding to the observed response, representing the equality or inequality of variances, was calculated, and compared with the F critical value under the null hypothesis of no effects, F_{crit}.

For this study, the null hypothesis equals the absence of a measurable variation on the surrounding soil shear strength after construction of the aggregate piers. A 95% confidence interval (i.e., significance $\alpha = 5\%$) for the evaluation of statistical significance was selected. When F_{crit} value is higher than F, the null hypothesis is not rejected. Also, the probability value, p-value, is used to accept or reject the null hypothesis. If the p-value is larger than the defined significance, the null hypothesis is accepted. Tables 4 and 5 show the results obtained from the ANOVA analyses. The F value and the p-value both conclude that the null hypothesis can't be rejected. These results do not contradict the design methodology, but it is important to take this into consideration during the design of aggregate piers.

This may not be applicable for softer soils, where the native site soil experiences more lateral displacement during installation. Figure 25 compares the results of this study (inclinometer I1 in F1 test) with those measured by White et al. (2007) in an inclinometer located 0.31 m from the edge of a pier under a concrete footing supported by a total of four aggregate piers. The average undrained shear resistance in White et al. (2007) was 30 kPa in comparison to the average undrained shear resistance of about 150 kPa in this study. The maximum lateral displacement measured in this study is about 3.0 mm while the displacement from White et al. (2007) is about 9 mm, which could be attributed to the higher initial soil shear strength. As shown, the mechanical properties of the surrounding soil affect the response of the aggregate pier. Thus, similar tests should be done in coarse material and fine-grained material with different consistencies to develop a better understanding of the construction effect caused by the installation of the aggregate piers.

Author	Method	Research Method and Primary Focus
Algin and Gumus (2018)	Numerical Modeling	3D numerical modeling - installation effect by increasing friction angle of the surrounding soil
Halabian and Shamsabadi (2014)		3D hybrid PFC/finite difference modeling - Construction effects of a single RAP. Consider increment of lateral radial stress
Pham and White (2007)		Comparison of stress distribution, settlement and lateral deformation measured on full scale load tests
Halabian et al. (2010)		The dynamic response of RAP-supported foundations for different conditions of geometry and soil matrix properties. Dynamic stiffness of shallow foundations.
White et al. (2007)	Full Scale Field Testing	Vertical Stress distribution, stress concentration ratio, group efficiency, pier stiffness and lateral displacement
Lawton (2000)		Stress distribution between aggregate pier and soil matrix
Handy and White I and II (2006)		Increase in lateral stress during construction of the aggregate pier
Wissmann et al.		Stress-settlement response of aggregate piers during load test
Greenwood (1991)		Performance of stone columns for full-scale and single piers tests
Stuedlein and Holtz (2013)		Bearing capacity of spread footings supported by aggregate piers in cohesive soils

Table 2. Previous studies of aggregate piers

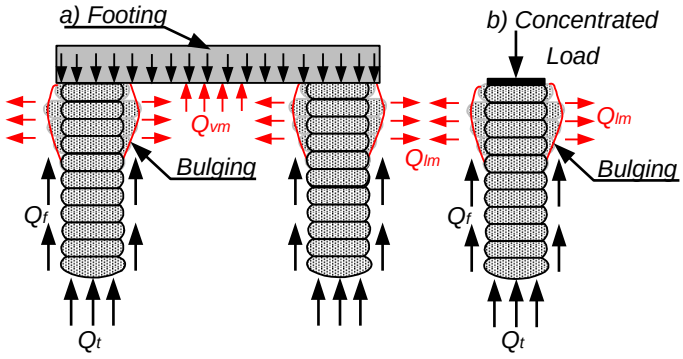

Figure 9. Stress distribution between aggregate pier and surrounding soil a) Group of piers under footing; b) Single pier

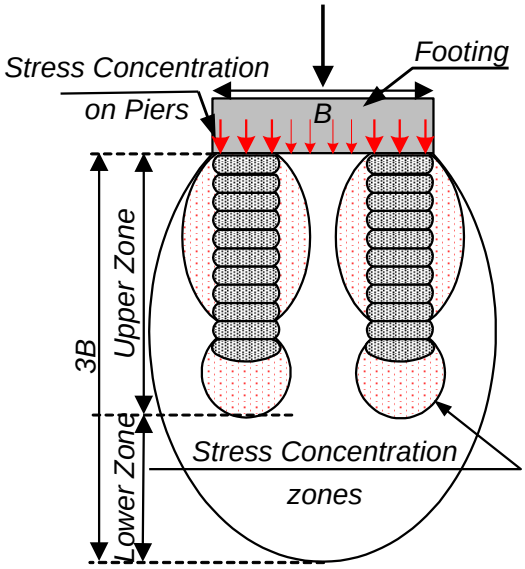

Figure 10. Settlement analysis procedure

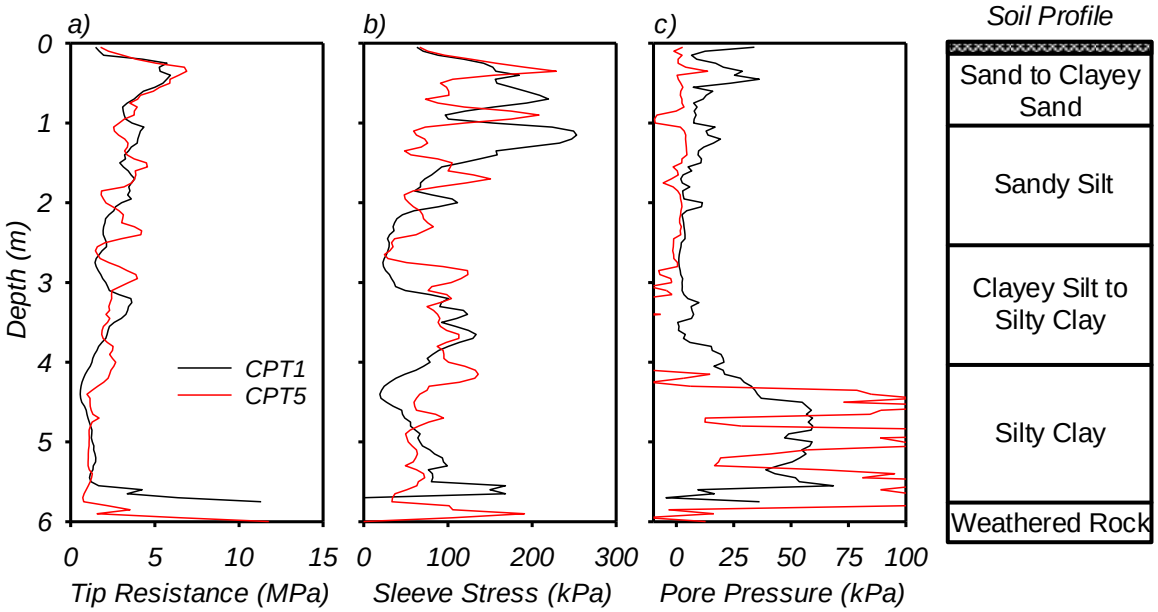

Figure 11. CPT initial conditions

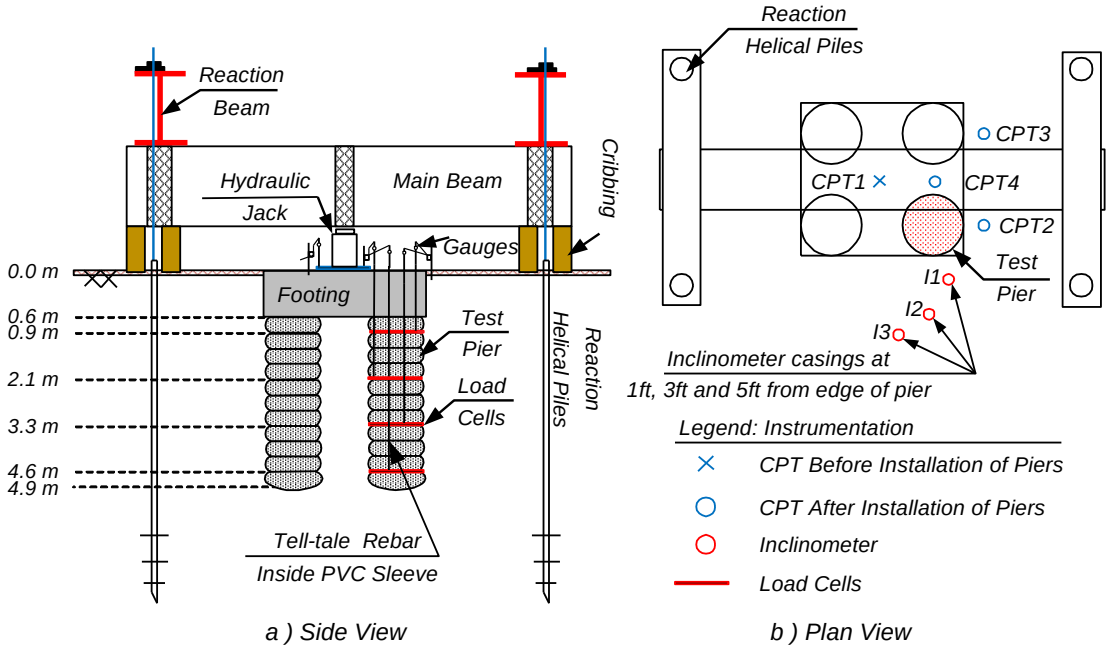

Figure 12. Schematic of the full-scale load test

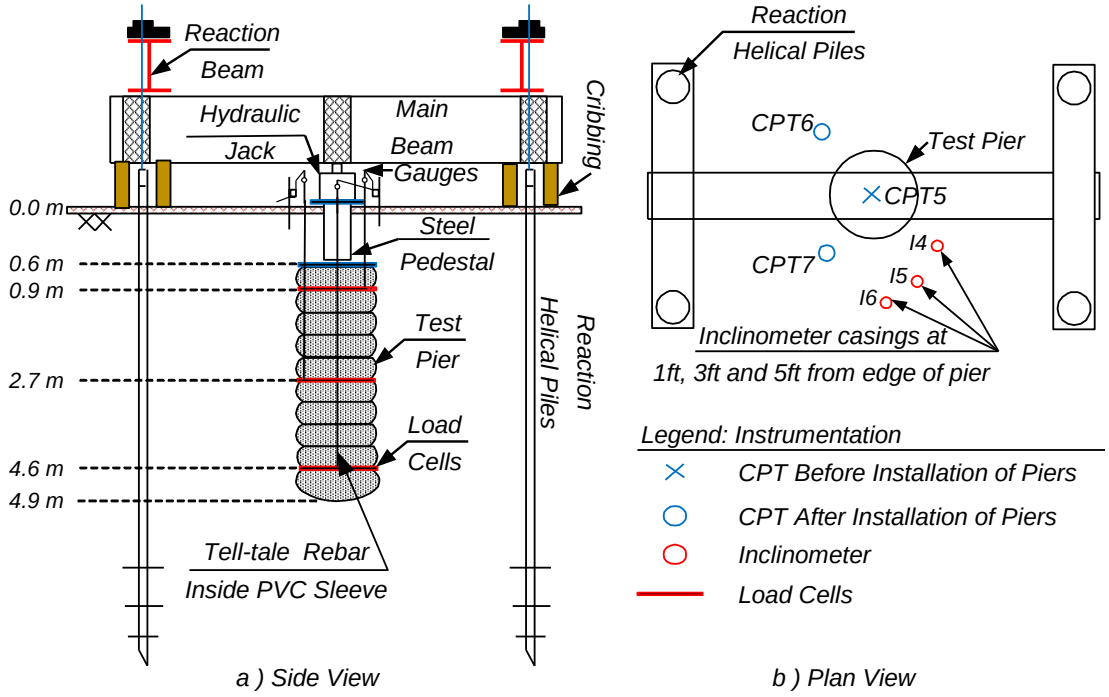

Figure 13. Schematic of the single pier load test

Element	Unit Weight γ (kg/m3)	c' (kPa)	ϕ'
Aggregate Pier	2140	1.0	52

Table 3. Material used to build the aggregate piers

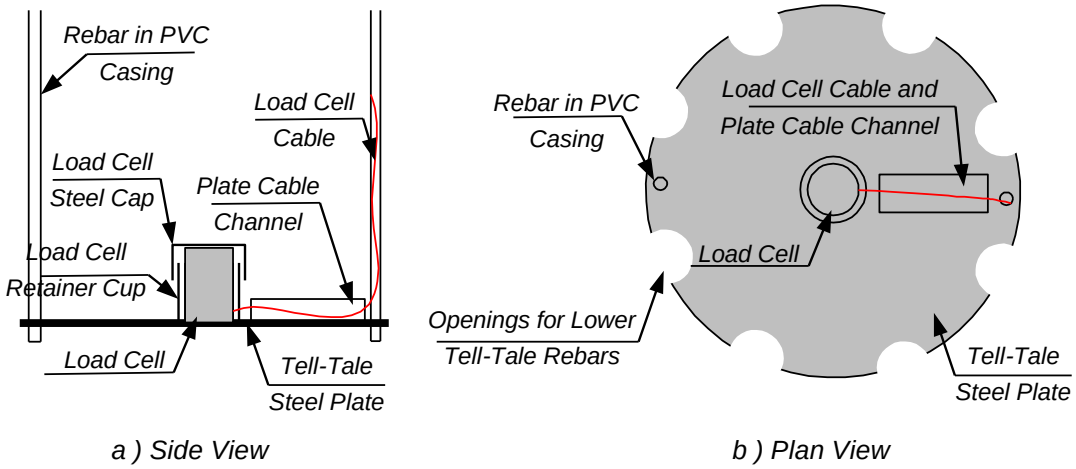

Figure 14. Tell-tale reference plate

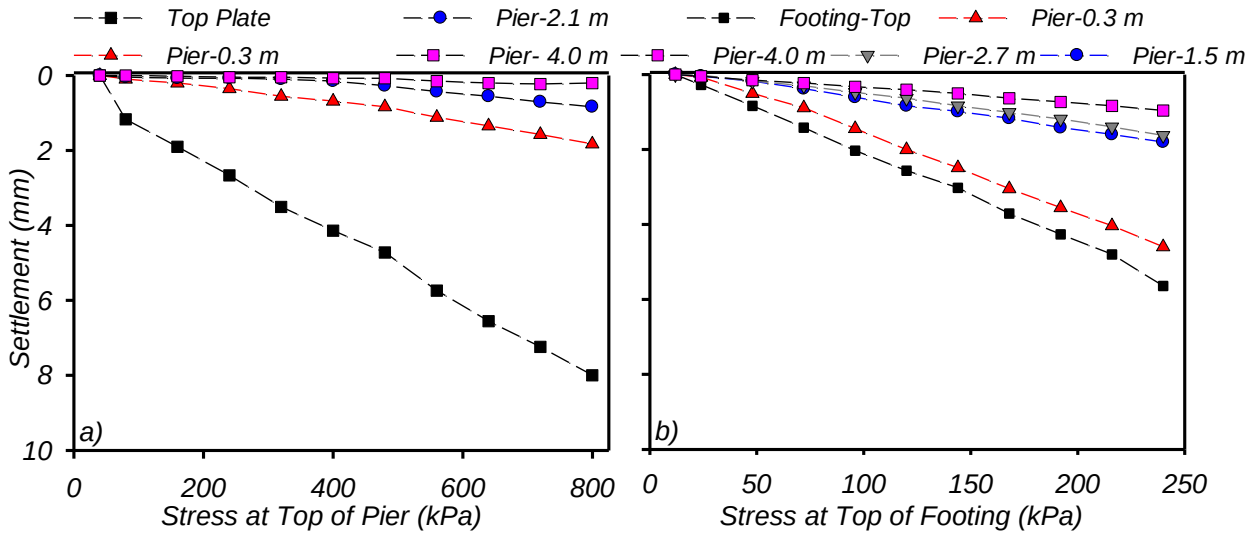

Figure 15. Measured load-settlement curves for: a) Single pier test; b) Concrete footing test

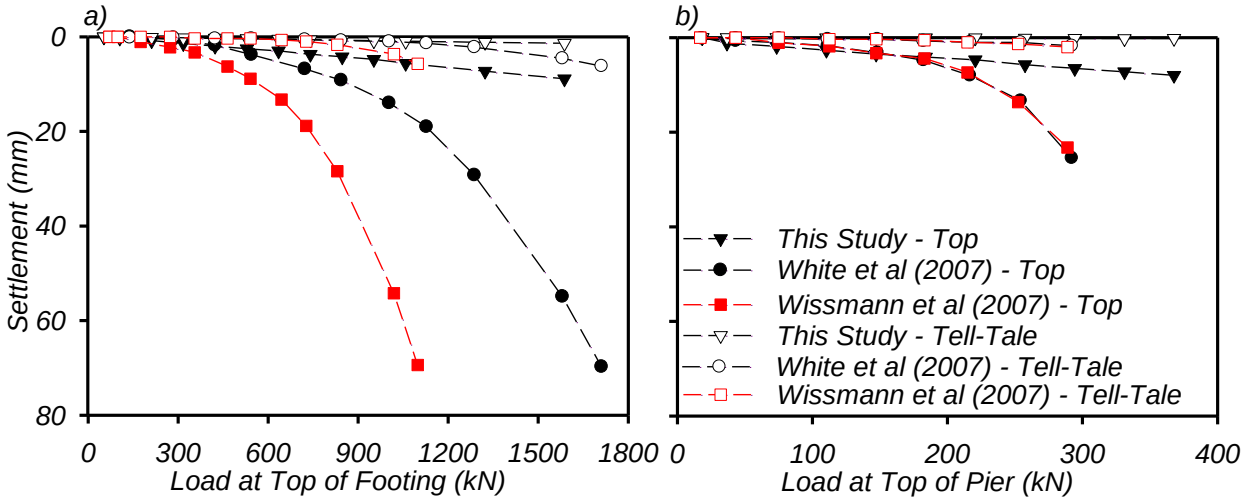

Figure 16. Comparison of the measured Load-Settlement Curves for: a) Footing Test; b) Single Pier Test

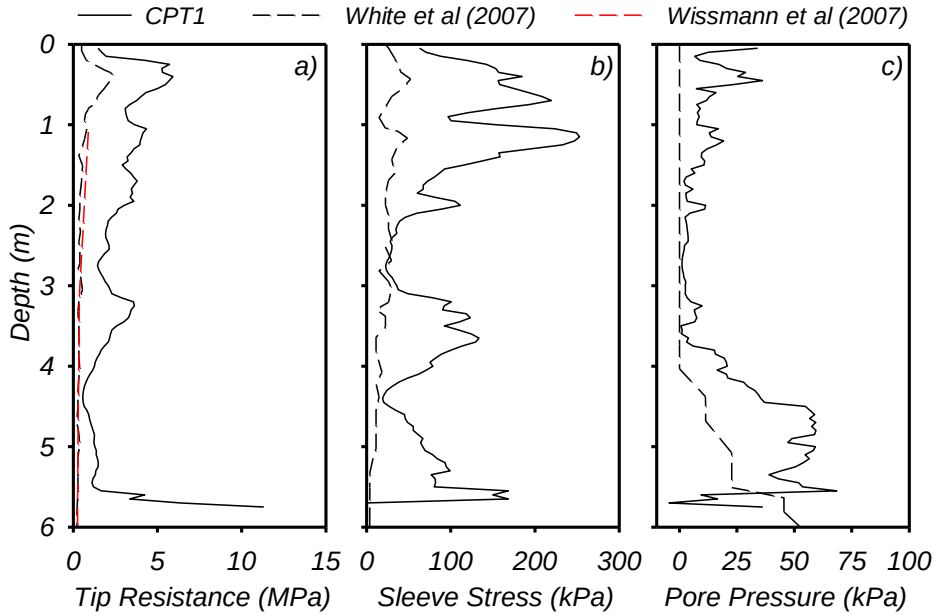

Figure 17. Comparison of CPT initial conditions

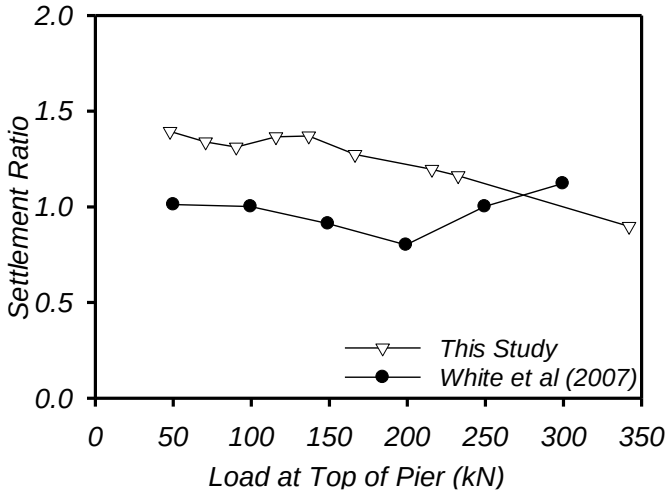

Figure 18. Group efficiency

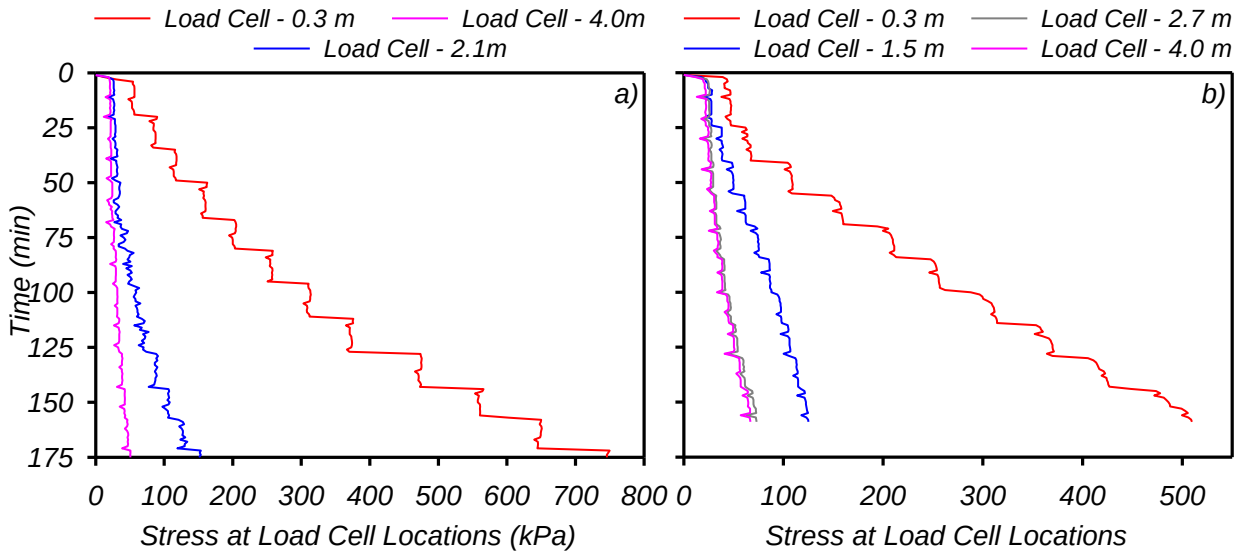

Figure 19. Vertical stress distribution: a) Single pier; b) Footing test

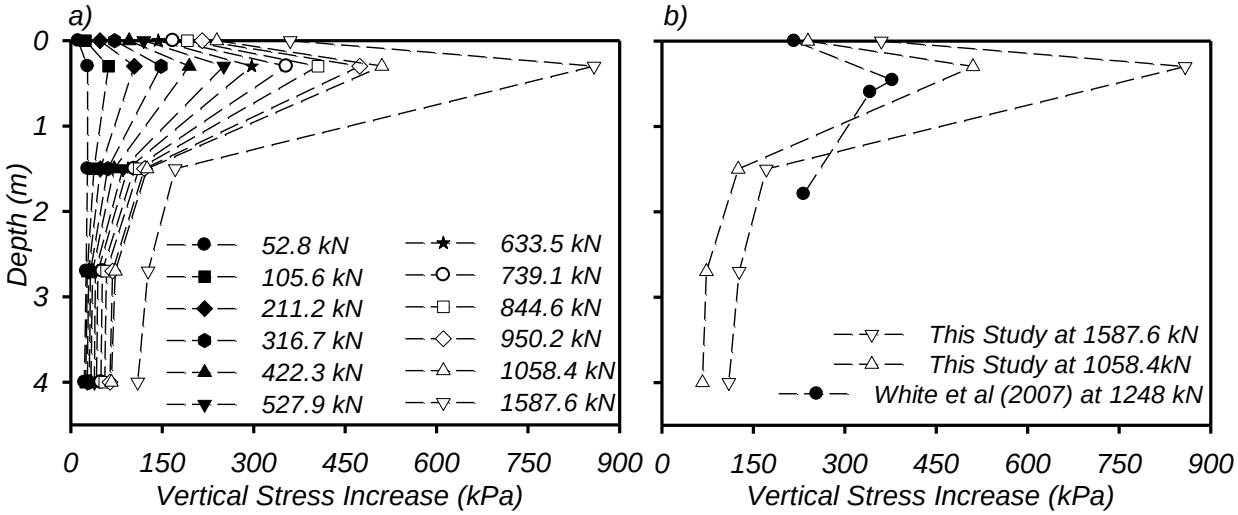

Figure 20. Vertical stress increase at each load cell a) Footing test; b) Comparison

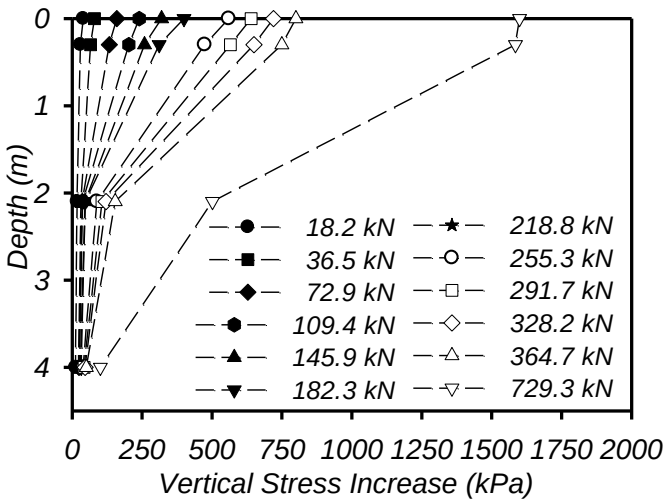

Figure 21. Single pier vertical stress increase at each load cell

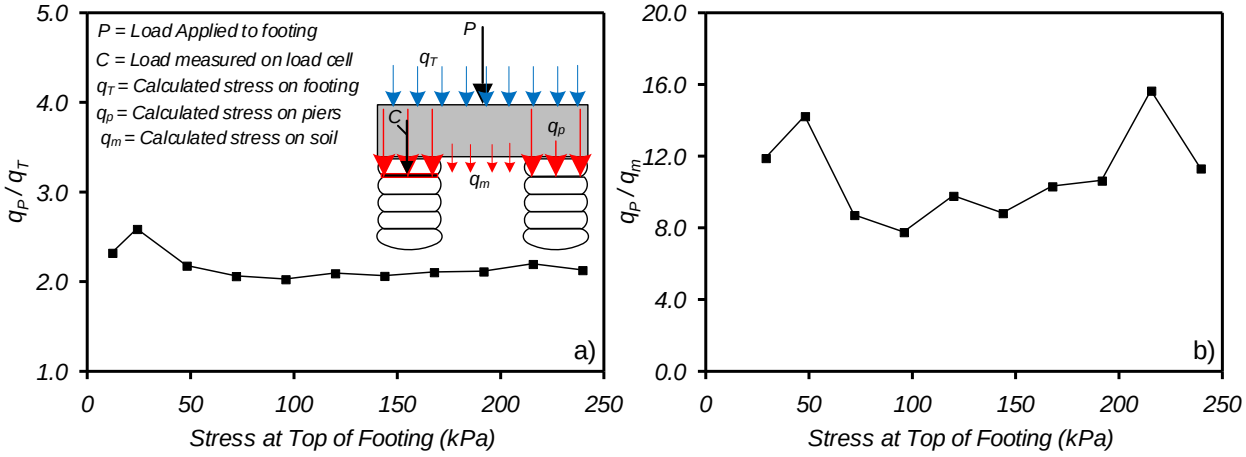

Figure 22. Stress concentration effect: a) Stress concentration b) Stress concentration ratio

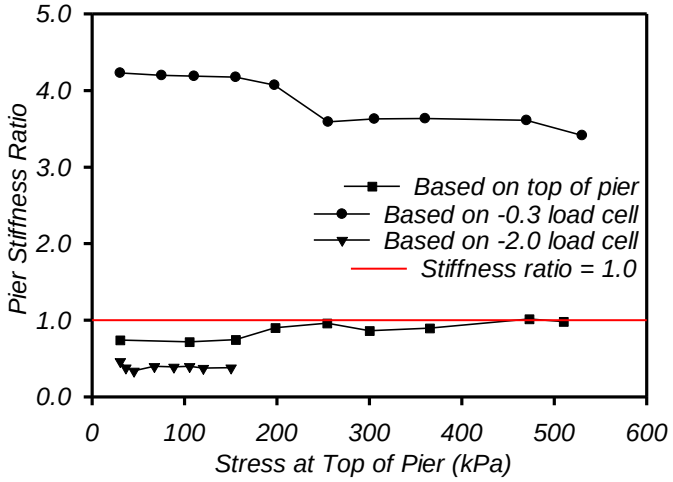

Figure 23. Pier stiffness ratio

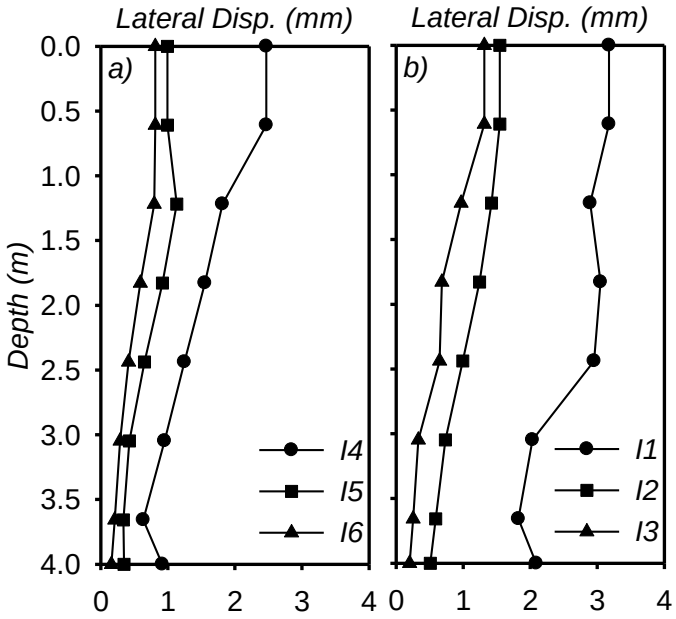

Figure 24. Inclinometer lateral deformation after installation a) Single pier test; b) Concrete footing.

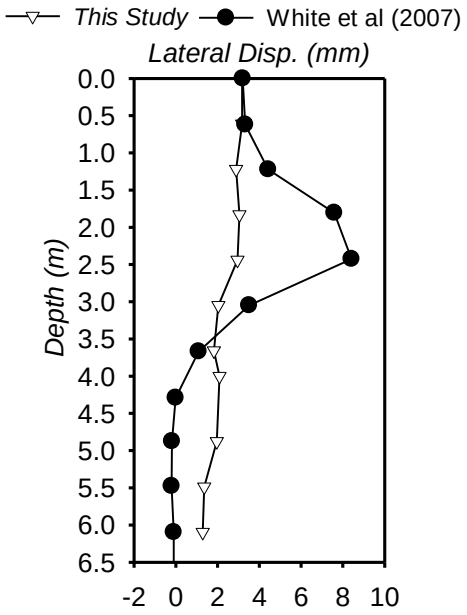

Figure 25. Comparison of lateral displacement after construction

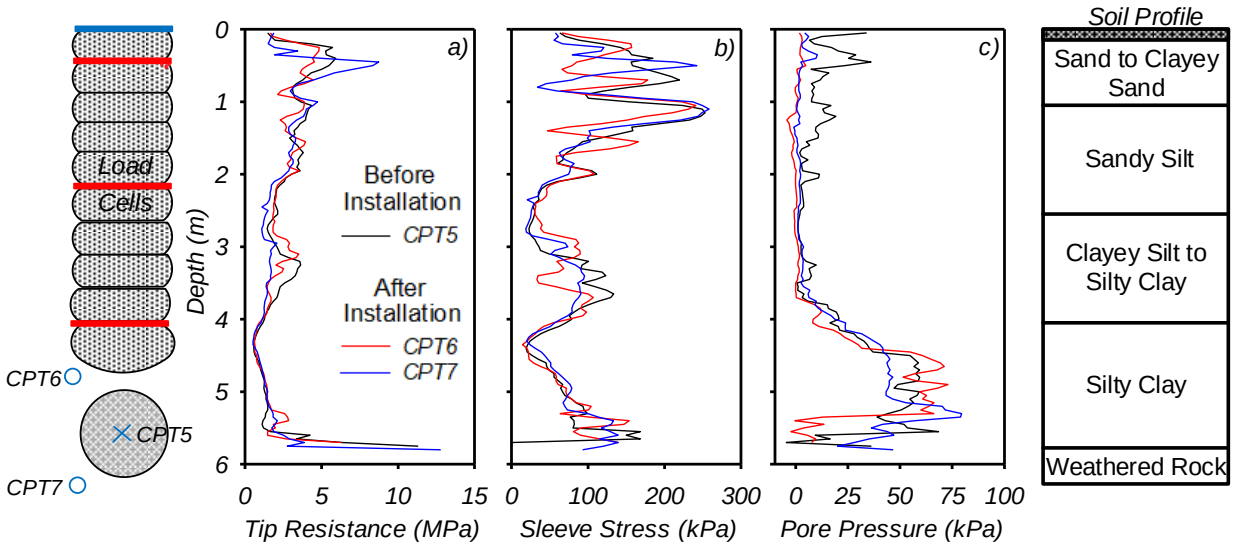

Figure 26. CPT prior and after installation of single aggregate pier

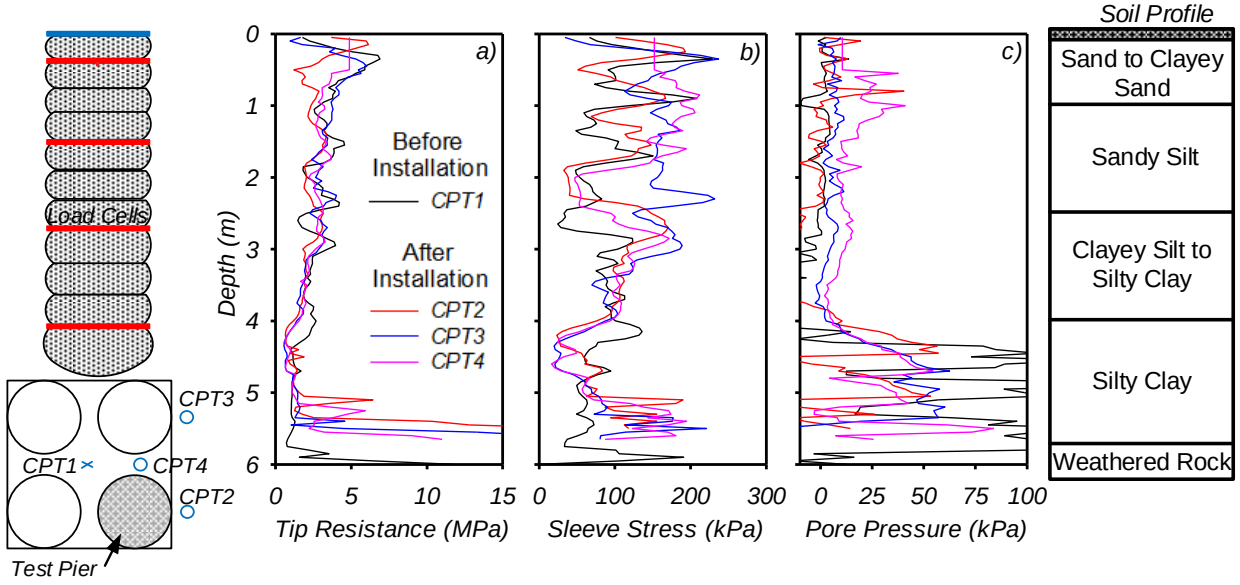

Figure 27. CPT prior and after installation of group of aggregate piers

CPT in Footing Test Zone				
Groups	*Count*	*Sum*	*Average*	*Variance*
CPT1	102	259110.6761	2540.30	1338229.41
CPT2	102	248536.8017	2436.63	5713044.28
CPT3	102	254211.5689	2492.27	1584534.89
CPT4	102	247107.0974	2422.62	1071839.19

Source of Variation	*SS*	*df*	*MS*	*F*	*P-value*	*F crit*
Between Groups	893663.05	3	297887.68	0.12274	0.9467	2.627
Within Groups	980472424.9	404	2426911.94			
Total	981366087.9	407				

Table 4. ANOVA Analysis for CPT tip resistance, Footing Test

CPT in Single Pier Test Zone				
Groups	*Count*	*Sum*	*Average*	*Variance*
CPT5	114	285389.2725	2503.414671	1847839.743
CPT6	114	266288.8832	2335.867396	1275710.377
CPT7	114	251063.9213	2202.315099	2146881.046

Source of Variation	*SS*	*df*	*MS*	*F*	*P-value*	*F crit*
Between Groups	5189631.795	2	2594815.898	1.4770	0.2298	3.022
Within Groups	595558721.8	339	1756810.389			
Total	600748353.6	341				

Table 5. ANOVA Analysis for CPT tip resistance, Single Pier Test

CHAPTER FIVE: SUMMARY AND CONCLUSIONS

This thesis is based on two different studies. The first one presents results of a numerical study that used a finite difference model to compare results obtained from modulus load tests with results of a numerical analysis. The 2D numerical analyses were shown to reasonably predict the aggregate pier load-deflection responses with the friction angle of the aggregate pier in the range of 48° to 52°. A series of parametric studies found that the friction angle of the aggregate pier could make a significant difference on the resulting settlement. A decrease of the friction angle by about 10% (keeping all other mechanical properties constant) could cause an increase on the expected settlement of up to 50%. In addition to the pier's friction angle, lateral stress was found to have a significant effect on the settlement analysis. During the field test, it was found, based on the DPT testing blow count, that the fines content within the material used for the construction of the aggregate piers can change the compaction percentage. As a result, there is a higher densification and a higher friction angle for the material with lower fines content.

The second study included two different load tests on aggregate piers. The first test was a full-scale instrumented load test performed on one trial square footing supported by four aggregate piers of 4.3 m long. To compare the results and the effect of the aggregate piers working together with the surrounding soil, one isolated pier of the same diameter and length as those in the group was also constructed and tested at the same site. Interpretations of the test results focus on the load-deformation behaviors of the piers, load transfer along pier shaft, stress distribution underneath the footing, group effect and the construction effect.

Major findings from this study include the following:

1. At a depth of about 3 diameters of the pier, the stress is about 25% of the stress measured at the -0.3 m load cell for both F1 and P1 tests.

2. The mode of deformation and its location during loading could be well recognized from the stress-settlement curves obtained from tell-tale reference plates. For both the P1 and F1 tests, there was lateral movement (e.g., bulging), in the matrix soil around the pier. Bulging depth increases with footing width.

3. The group efficiency was about 1.5 for lower stress applied to the top of the piers and decreased to a value of about 1.0 at the design load level.

3. The stress concentration ratio was found to range between 8 to 16 for the different applied stresses. Vertical compressive stress applied to the top of the pier was found to dissipate more rapidly along the shaft of the single pier compared to the group of piers.

4. The stiffness of piers varies with depth. In the upper part of the pier (e.g., 0.3 m below the surface), the single pier presents higher stiffness values while at lower elevations (e.g., 2.0 m below the surface), the group of piers present higher stiffness values. In average, however, the total stiffness ratio at the surface is around 1.0, suggesting that the stiffness measured on a single pier test could be considered representative of the stiffness of the piers within the group of piers supporting an isolated concrete footing.

4. The most notable lateral soil displacement during construction was extended to a depth of about 2.5 times the diameter of the pier. The lateral displacement appears not to be large enough to increase or modify the shear strength of the surrounding soil.

5. The statistical significance of the installation effects on the strength properties of surrounding soil were assessed using ANOVA analyses focused on tip resistance. The analysis concluded that

installation does not significantly change properties of the on-site surrounding soil. These results do not contradict the design methodology, but it is important to take this into consideration during the design of aggregate piers. It may not be applicable for softer soils where the native site soil experiences more lateral displacement during installation.

Recommendations for Further Study

Some recommendations for further research are as follows:

1. The tests performed in Chapter 3 were done in a medium stiff clay soil. As was shown in comparison to White et al. (2007) and Wissmann et al. (2007), the mechanical properties of the surrounding soil greatly affect the response of the aggregate pier. Thus, similar tests should be done in coarse material and fine-grained material with different consistencies to have a better understanding of the stress-transfer mechanism of the aggregate piers.

2. Inclinometer and CPT testing after installation should be done in fine grained material and coarse material with different consistencies to have a better understanding of the construction effect of the aggregate piers.

3. Horizontal displacement during consolidation should be measured.

4. Vertical stress distribution along the pier shaft and the stress concentration ratio of aggregate piers should be measured for different applications (e.g., embankment, storage tank, and floor slab support).

REFERENCES CITED

REFERENCES CITED

Algin, H. M., and Gumus, V. (2018). “3D FE Analysis on Settlement of Footing Supported with Rammed Aggregate Pier Group.” Int. J. Geomech., 2018, 18(8), 10.1061/(ASCE)GM.1943-5622.0001189.

Ashmawy, A.K., Rokicki, R., and Plaskett, M.E. (2000) "Predicted and Actual Settlement of Soils Improved By Vibro Replacement," Advances in Grouting and Ground Modification, Proceedings of Geo-Denver 2000, GSP No. 104, Krizek, R.J., and Sharp, K., ed.s, ASCE, Reston, Virginia.

Bachus, R.C., and Barksdale, R.D. (1984) "Vertical and Lateral Behavior of Model Stone Columns," Proceedings, In Situ Soil and Rock Reinforcement, Presses de l'ecole de nationale des Ponts et Chaussees, Paris, France.

Balaam, N.P., and Poulos, H.G. (1978). "Methods of analysis of single stone columns”. Proceedings of the Symposium on Soil Reinforcing and Stabilizing Techniques, Australia, 497-512.

Balaam, N.P., and Brooker, J.R. (1981). "Analysis of rigid rafts supported by granular piles." International Journal for Numerical and Analytical Methods in Geomechanics, 5, 379-403.

Barksdale, R.D., and Bachus, R.C. (1983a) "Design and Construction of Stone Columns," Vol. 1, Report No. FHWA/RD 83/026, Federal Highway Administration.

Barksdale, R.D., and Bachus, R.C. (1983b) "Design and Construction of Stone Columns," Vol. 2, Report No. FHWA/RD 83/026, Federal Highway Administration.

Barksdale, R.D., and Goughnour, R. (1984) "Settlement Performance of Stone Columns," Proceedings, In Situ Soil and Rock Reinforcement, Presses de l'ecole de nationale des Ponts et Chaussees, Paris, France.

Bergado, D.T., and Lam, F.L. (1987b) "Full Scale Load Test of Granular Piles with Different Densities and Different Proportions of Gravel and Sand in the Soft Bangkok Clay," Soils and Foundations Journal, Vol. 27, No. 1, Japan. 86-93.

Bergado, D.T., Anderson, L.R., Miura, N., and Balasubramaniam, A.S. (1996) "Chapter 5: Granular Piles," Soft Ground Improvement in Lowland and Other Environments, ASCE Press, New York.

Bergado, D.T., Huat, S.H., and Kalvade, S. (1987a) "Improvement of Soft Bangkok Clay Using Granular Piles in Subsiding Environment," Proceedings, 5th International Geotechnical Seminar on Case Histories in Soft Clay, Singapore. 219-226.

REFERENCES CITED

Bergado, D.T., Rantucci, G., and Widoso, S. (1984) "Full Scale Load Tests of Granular Piles and Sand Drains in the Soft Bangkok Clay," Proceedings, In Situ Soil and Rock Reinforcement, Presses de I'ecole de nationale des Ponts et Chaussees, Paris, France.

Braja, M.D., Nagaratnam, S., (2019). Principles of Foundation Engineering. (Ninth Edition). 2016 Cengage Learning, Inc.

Brauns, J. (1978) "Initial Bearing Capacity of Stone Columns and Sand Piles," Soil Reinforcing and Stabilizing Techniques in Engineering Practice, Sydney, Vol. I., 497-512.

Caskey, J.M. (2001). Uplift Capacity of Rammed Aggregate Pier Soil Reinforcing Elements. M.Sc. Thesis, University of Memphis, Memphis, TN, USA.

Charles, J.A., and Watts, K.S. (1983) "Compressibility of Soft Soil Reinforced with Granular Columns," Improvement of Ground, Proceedings of The Eighth European Conference on Soil Mechanics and Foundations Engineering, Rathmayer, H.G., and Saari, K.H.O., eds., Balkema, Rotterdam, The Netherlands. 347-352

Chen, J.-F., Han, J., Oztoprak, S., and Yang, X.-M. (2009). “Behavior of single rammed aggregate piers considering installation effects.” Comput. Geotech., 36(7), 1191–1199.

Clemente, J.L., and Davie, J.R. (2000) "Stone Columns for Settlement Reduction," Proceedings, GeoEng 2000, Melbourne, Australia

Clemente, J.L.M., Senapathy, H. and Davie, J.R. (2005) "Performance Prediction of Stone Column-Supported Foundations," Proceedings, Sixteenth International Conference on Soil Mechanics and Geotechnical Engineering, Osaka, Japan. 1327-1330

Datye, K.R., and Nagaraju, S.S. (1975) "Installation and Testing of Rammed Stone Columns," Proceedings, IGS Specialty Session, 5th Asian Regional Conference on Soil Mechanics and Foundation Engineering, Bangaladore, India. 101-104

Davis, C.A. and Roux, R.F. (1997) "Case Study: Stone Columns for Controlling Differential Settlement," Ground Improvement, Ground Reinforcement, Ground Treatment, Developments 1987-1997, GSP No. 69, ASCE; V. Schaefer, Ed.; Reston, VA.

Engelhardt, K., and Golding, H.C. (1975) "Field Testing to Evaluate Stone Column Performance in a Seismic Area," Geotechnique, Vol. 25, No. 1, Thomas Telford Ltd., London, UK.

Fox, N.S., and Cowell, M.J. (1998). “Geopier™ Soil Reinforcement Manual.” Geopier™ Foundation Company, Blacksburg, Virginia.

REFERENCES CITED

FitzPatrick, B.T., Wissmann, K.J., and White, D.J. (2003) "Settlement Control for Embankments and Transportation-Related Structures Using Geopiers Soil Reinforcement," Technical Bulletin No. 6, Geopier Foundation Company, Inc.

Goughnour, R.R., and Bayuk, A.A. (1979a) "Analysis of Stone Column-Soil Matrix Interaction Under Vertical Load," Proceedings of the International Conference on Soil Reinforcement: Reinforced Earth and Other Technologies, Vol. I, Paris, France. 271-277

Goughnour, R.R., and Bayuk, A.A. (1979b) "A Field Study of Long Term Settlements of Loads Supported by Stone Columns in Soft Ground," Proceedings of the International Conference on Soil Reinforcement: Reinforced Earth and Other Technologies, Vol. I, Paris, France. 279-285

Goughnour, R.R. (1983) "Settlement of Vertically Loaded Stone Columns in Soft Ground," Improvement of Ground, Proceedings of The Eighth European Conference on Soil Mechanics and Foundations Engineering, Rathmayer, H.G., and Saari, K.H.O., eds., Balkema, Rotterdam, The Netherlands. 235-240.

Greenwood, D.A. (1970) "Mechanical Improvement of Soils Below Ground Surface," Proceedings, Conference on Ground Engineering, Institution of Civil Engineers, London, UK.

Greenwood, D.A. (1991) "Load Tests on Stone Columns," Deep Foundation Improvements: Design Construction and Testing, Special Testing Publication 1089, Esrig, M. I., and Bachus, R. C, ed.'s, American Society for Testing and Materials, Philadelphia

Greenwood, D.A., and Kirsch, K. (1984) "Specialist Ground Treatment by Vibratory and Dynamic Methods," State of the Art Report, Piling and Ground Treatment, Thomas Telford Ltd., London, UK. 17-45

Halabian, A. M., Naeemifar, I., and Hashemolhosseini, S. H. (2012a). “Numerical analysis of vertically loaded rammed aggregate piers and pier groups.” Proc. Inst. Civ. Eng., 165(3), 167–181.

Halabian, A. M., and Shamsabadi, P.J. (2014). “Numerical Modeling of the RAP Construction Process and Its Effects on RAP Behavior.” Int. J. of Geomechanics, 15(5), 10.1061/(ASCE)GM.1943- 5622.0000429.

Handy, R.L. (2001). "Does lateral really influence settlement?" Journal of Geotechnical and Geoenvironmental Engineering, ASCE, 127(7), 623-626.

REFERENCES CITED

Handy, R. L., and White, D. J. (2006a). “Stress zones near displacement piers. I: Plastic and liquefied behavior.” J. Geotech. Geoenviron. Eng.

Handy, R. L., and White, D. J. (2006b). “Stress zones near displacement piers. II: Radial cracking and Wedging.” J. Geotech. Geoenviron. Eng.

Hoevelkamp, K. K. (2002). “Rammed aggregate pier soil reinforcement: Group load tests and settlement monitoring of large box culvert.” MS thesis, Iowa State Univ., Ames, Iowa.

Hughes, J.M.O., and Withers, N.J. (1974). "Reinforcing of soft cohesive soils with stone columns." Ground Engineering, 7(3), 42-49.

Hughes, Withers, N.J., and Greenwood, D.A. (1975). "A field trial of the reinforcing effect of a stone column in soil." Geotechnique, 25(1), 31-44.

Hussin, J.D., and Baez, J.I. (1991) "Analysis of Quick Load Tests on Stone Columns: Case Histories," Deep Foundation Improvements: Design Construction and Testing, Special Technical Publication 1089, Esrig, M. I., and Bachus, R. C, ed.'s, American Society for Testing and Materials, Philadelphia

Hvorslev, M.J. (1949) "Subsurface exploration and sampling of soil for civil engineering purposes," U.S. Waterways Experiment Station, Vicksburg, Mississippi. 521 p.

Hvorslev, M.J. (1960) "Physical Components of the Shear Strength of Saturated Clays," Proceedings, ASCE Research Conference on the Shear Strength of Cohesive Soils, Boulder, 169-173.

Lawton, E. C., and Fox, N. S. (1994). “Settlement of structures supported on marginal or inadequate soils stiffened with short aggregate piers.” Proc., Vertical and Horizontal Deformations of Foundations and Embankments, Geotechnical Special Publication No. 40, ASCE, College Station, Tex., Vol. 2, 962–974.

Lawton, E. C., Fox, N. S., and Handy, R. L. (1994). “Control of settlement and uplift of structures using short aggregate piers.” Proc., In-Situ Deep Soil Improvement, Vol. 45, ASCE, Reston, VA, 121–132.

Lawton, E.G., and Warner, B.J. (2004). Performance of a group of Geopier elements loaded in compression compared to single Geopier elements and unreinforced soil. Final Report, Report No. UUCVEEN 04-12, University of Utah, Salt Lake City, UT, USA.

REFERENCES CITED

Lee, J.S., and Pande, G.N. (1998). "Analysis of stone-column reinforced foundations." International Journal for Numerical and Analytical Methods in Geomechanics, 22, 1001-1020.

Kurt, E., and Teymur, B., (2012). “Comparison of the results of load test done on stone columns and rammed aggregate piers using numerical modeling.” 3rd International Conference on New Developments in Soil Mechanics and Geotechnical Engineering, 28-30 June 2012, Near East University, Nicosia, North Cyprus.

Minks, A.G., Wissmann, K.J., Caskey, J.M., and Pando, M.A. (2001). "Distribution of stresses and settlements below floor slabs supported by rammed aggregate piers." Proceedings of the 54th Canadian Geotechnical Conference, Calgary, Canada, September 16-19.

Mitchell, J.K. (1981). "Soil improvement: State-of-the-art." Proceedings of the 10th International Conference on Soil Mechanics and Foundation Engineering, Stockholm, Sweden, 4, 509-565.

Mitchell, J.K., and Huber, T.R. (1985). "Performance of stone column foundation”. Journal of Geotechnical Engineering, ASCE, 111(2), 205-223.

Mohammadi, S. D., Nikoudel, M.R., Rahimi, H., Khamehchiyan, M. (2008) “Application of the Dynamic Cone Penetrometer (DCP) for determination of the engineering parameters of soils.” Engineering Geology 101 (2008) 195–203

Pham, H. (2005). “Support mechanism for rammed aggregate pier.” Ph.D. dissertation, Iowa State Univ., Ames, IA.

Robertson, P.K., and Campanella, R.G. (1986). Guidelines for use, interpretation, and application of the CPT and CPTU. 3rd Eds., Hogentogler and Co., Inc.

Stuedlein, A., Holtz, R., (2013). “Bearing Capacity of Spread Footings on Aggregate Pier Reinforced Clay”. Journal of Geotechnical and Geoenvironmental Engineering DOI: 10.1061/(ASCE)GT.1943-5606.0000748

Suleiman, M. T., and White, D. J. (2006). “Load transfer in rammed aggregate piers.” Int. J. Geomech., 10.1061/(ASCE)1532-3641(2006)6:6(389), 389–398.

White, D.J., E.C. Lawton, and J.M. Pitt. (2000). “Lateral Earth Pressure Induced by Rammed Aggregate Piers.” Proceedings, 53rd Annual Canadian Geotechnical Conference. Montreal, Canada.

REFERENCES CITED

White, D. J., Suleiman, M. T., Pham, H. T., and Bigelow, J. (2002). “Constitutive equations for aggregates used in Geopier foundation construction.” Final Rep., Iowa State Univ., Ames, Iowa.

White, D. J., Wissmann, K. J., Barnes, A., and Gaul, A. (2002). "Embankment support: a comparison of stone column and rammed aggregate pier soil reinforcement". Proceedings of the 55th Canadian Geotechnical Conference, Niagara Falls, Ontario, Canada.

White, D. J., Gaul, A. J., and Hoevelkamp, K. (2003). “Highway applications for rammed aggregate pier in Iowa soils.” Final Rep., Iowa DOT TR-443, Ames, Iowa.

White, D. J., and Suleiman, M. T. (2005). “Design of short aggregate piers to support highway embankments.” Transportation Research Record, 1868. Transportation Research Board, Washington, D.C., 103–112.

White, D. J., Pham, H. T., and Wissmann, K. J. (2006). “Numerical simulation of construction-induced stresses around rammed aggregate piers.” Proc., Int. Conf. on Numerical Simulation of Construction Processes in Geotechnical Engineering for Urban Environment, NSC06, Bochum, Germany, 257–264.

White, K. J., Pham, H. T. V., and Hoevelkamp, K. K. (2007). “Support mechanisms of rammed aggregate piers. I: Experimental results.” J. Geotech. Geoenviron. Eng., 10.1061/(ASCE)1090-0241(2007)133: 12(1503), 1503–1511.

Wissmann, K.J. (1999). "Bearing capacity of Geopier-supported foundation systems." Technical Bulletin No. 2, Geopier Foundation Company, Inc., Blacksburg, VA, USA.

Wissmann, K.J., Fox, N.S., and Martin, J.P. (2000). "Rammed aggregate piers defeat 75-foot-long driven piles." Proceedings of Performance Confirmation of Constructed Geotechnical Facilities, Geotechnical Special Publication No. 94, ASCE, Amherst, MA, 198-210.

Wissmann, K. J., Moser, K., and Pando, M. (2001). “Reducing settlement risks in residual piedmont soil using rammed aggregate pier elements.” Proc., Foundations and Ground Improvement, Geotechnical Special Publication No. 113, ASCE, Blacksburg, Va., 943–957.

Wissmann, K. J., White, D.J., and Lawton, E. (2007). “Load Test Comparisons for Rammed Aggregate Piers and Pier Groups.” Univ. of Utah, Salt Lake City, Utah.

Wong D.O., FitzPatrick, B.T., and Wissmann, K.J. (2004). "Stabilization of retaining walls and embankments using rammed aggregate piers™." Proceedings of Geo-Trans 2004, Geotechnical Special Publication No. 126, ASCE, Los Angeles, CA, 1866 - 1875.

APPENDICES

APPENDIX A

PICTURES OF THE FULL-SCALE FIELD TEST CONSTRUCTION PROCESS


KOMATSU


CAT